Power-scavenging Tumbleweed Rover

Design, development, and testing of a Tumbleweed rover capable of generating electrical power by utilizing wind energy

by

Goran Jurisa Basic

A thesis submitted in conformity with the requirements
for the degree of Master of Applied Science
Graduate Department of Aerospace Engineering
University of Toronto

Abstract

Power-scavenging Tumbleweed Rover

Design, development, and testing of a Tumbleweed rover capable of generating electrical power by utilizing wind energy

Goran Jurisa Basic

Master of Applied Science

Graduate Department of Aerospace Engineering

University of Toronto

2010

Most current space robotics vehicles use solar energy as their prime energy source. In spherical robotic vehicles the use of solar cells is very restricted.

Focusing on the particular problem, an improved method to generate electrical power will be developed; the innovation is the use of an internal pendulum-generator mechanism to generate electrical power while the ball is rolling. This concept will enable spherical robots on future long-duration planetary exploration missions.

Through a developed proof-of-concept prototype, inspired by the Russian thistle plant, or tumbleweed, this thesis will demonstrate power generation capabilities of such a mechanism. Furthermore, it will also present and validate a parametric analytical model that can be used in future developments as a design tool to quantify power and define design parameters. The same model was used to define the design parameters and power generation capabilities of such a system in Martian environment.

Dedication

Dedicated to the people who inspired and enlightened my life in every way and especially my parents Karmen and Mladen, my beloved partner Ash, and my best friends Bruna, Minja and Chunky.

This is to honour your efforts in making me a better person and allowing me to follow my dreams. I love you all so much.

Acknowledgements

This thesis is a product of a hard work in the past two years. During that time, many people have contributed to its development through their generous support and advice.

Most importantly, I would like to express my gratitude to my supervisor Tim Barfoot who taught me how to think and see things in a different perspective. His guidance was precious and I could never have done it without his understanding.

Furthermore, I would also like to thank Jaret Matthews for the things he taught me and for priceless experiences I gained through working with him.

I would also like to mention the unselfish support of my colleagues Keith and Chi who spent lots of their own time and energy in discussing issues and giving me absolutely invaluable ideas.

Also, I would like to thank my very close friends Navtej and Hassan who spent countless hours discussing physics or giving me invaluable moral support and helping me understand the concepts beyond my imagination.

I would like to thank Billy, our summer student of 2010, and Andrew who helped me perform the field experiments and provided an important support when needed most.

Lastly, I would like to express my thanks to everybody whom I may have forgotten at this late hour, but have provided me with their support, energy and inspiration.

Thank you.

Goran Basic, August 2010.

Contents

List of Tables

List of Figures

Chapter 1

Introduction

1.1 Motivation

Ball shaped rovers in robotics have been studied with great interest due to their unique shape characteristic that gives them some very interesting and peculiar features compared to rovers utilizing other locomotion concepts. Looking closely, we can see many similar features to ball robots in nature. For example, plants have been using wind propulsion in many creative ways but mostly for spreading seeds and some of them even as a transportation system [8]. One such plant is a Tumbleweed plant, shown in Figure 1.1, which inspired robot designers to envision the Tumbleweed rover [33, 25, 6]. A tumbleweed plant is unique due to its ability to distribute its seeds and by being blown around the desert propelled by wind covering enormous distances. Several ball robot designs seek to imitate the tumbleweed plant, as will be discussed later in this thesis.

The Tumbleweed rover concept was first conceived by Jacques Blamont of the National Center for Space Studies (CNES Centre National d'Etudes Spatiales) in France in 1977 for use on Mars. Blamont's concept was a 3-10 m diameter inflatable ball that could carry payloads of 20-30 kg for distances of approximately 100 km, driven by the wind or powered by an inner drive mechanism [4].

Tumbleweed rover technology was envisioned to provide a reliable and low-cost solution for gathering science data over vast areas, applicable to both terrestrial and extraterrestrial applications. Furthermore, a Tumbleweed rover could also be a very economical way to deploy various instruments on planetary surfaces. Taking into account data gathered on previous missions to Mars, it was calculated that a Tumbleweed rover 6 m in diameter, weighing 20 kg, carrying 20 kg payload, and propelled by wind power, could be large enough to achieve mobility on Mars [19]. This assumption was based on geology and topography of the Martian surface, which is quite a favourable environment and such performance is sufficient enough to traverse some 99% of the Martian surface.

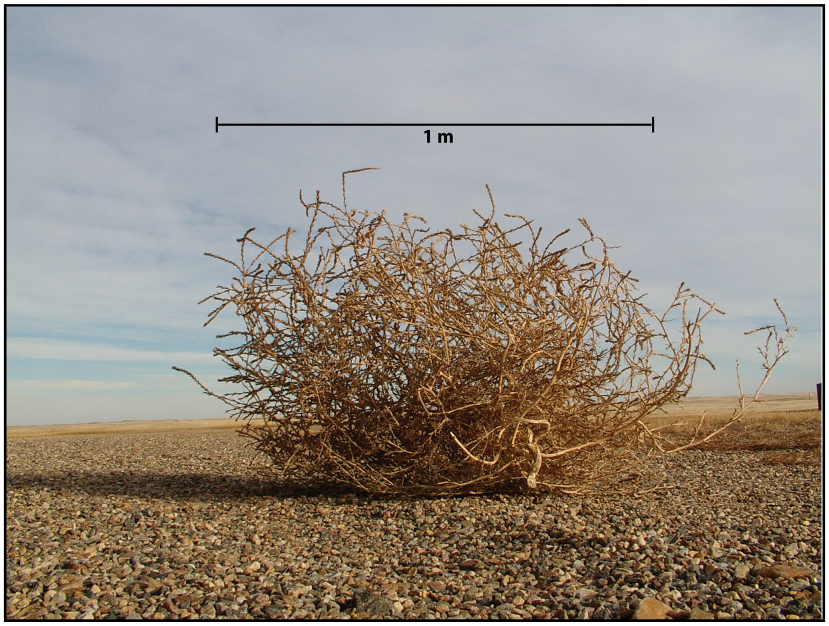

Figure 1.1: Tumbleweed plant

Over the years, it was also concluded that there are spherical structural configurations that would achieve higher drag coefficients than plain spherical ones providing even better performance [7]. Some of this analysis will be covered later in more detail. As we can see, Tumbleweed rover technology is very promising due to its unique characteristics. However, there is one major drawback. Having a spherical shell mandates that the payload and the whole robot body must be enclosed within it. This, of course, imposes a serious problem on power generation and payload deployment on such a vehicle. Furthermore, this severely reduces autonomy and feasibility.

In the majority of space missions, solar cells are most commonly used and are the most reliable way to generate power on a spacecraft. Because of the Tumbleweed's spherical characteristics, solar cells would be quite useless if integrated inside the shell and prone to destruction if integrated outside the shell, which is in constant contact with the ground. Furthermore, solar cells are also very dependable on solar flux and incidence angle, which can be easily obscured by dust, storms or even ice. A good example is the recently decommissioned Phoenix Lander on Mars, which stopped communicating with ground stations due to ice collecting on the solar cells [3].

The concept proposed in this work provides a robust and reliable solution for Tumbleweed power generation. The proposed solution is only dependent on the wind for its propulsion and power generation and is not affected by any unfavourable meteorological phenomena compared to solar cells.

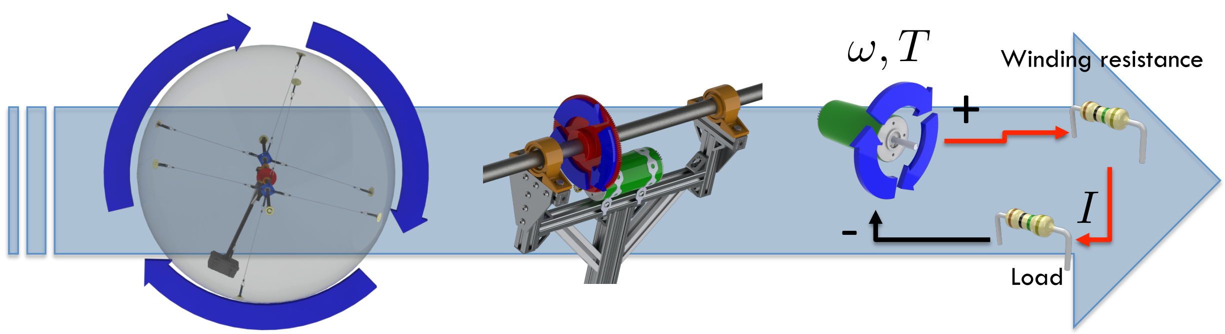

Figure 1.2: Proposed solution

The proposed solution, depicted in Figure 1.2, uses a pendulum inside an inflatable spherical shell to generate power. Similar to a windmill, when a ball is being pushed by the wind, the pendulum rotates around the main axle and acts on the generator through a geared mechanism. This creates electrical power that is measured through the sensors located in the payload box. The details of the design will be covered in more detail in later sections.

Many research efforts have been undertaken in the United States at Jet Propulsion Laboratory (JPL), Langley Research Center (LaRC) and North Carolina State University (NCSU). In Europe, Tumbleweed technology developments were undertaken by the Helsinki University of Technology and Swiss Federal Institute of Technology (EPFL) in Lausanne. Two different technology development pathways have been the basis of Tumbleweed technology evolution: LaRC, NCSU and Helsinki University of technology have performed work on Tumbleweeds with deployable structures, while JPL's concept utilizes inflatable shells [4, 10].

1.2 Objectives

Motivated by the problem of power generation in robots for space exploration and the requirements that such spherical rover concepts impose on the design, this work focuses on developing a method to efficiently harvest wind energy. In order to understand all the factors impacting the capability of power generation, a prototype was developed and tested. Relationships between different design parameters will be explained and such prototype will allow us to easily scale the design for operations in any planetary environment.

The project was executed in several phases and following objectives have been accomplished:

1. Development of a parametric analytical model for Tumbleweed ball rover capable of generating electrical power with a pendulum while being propelled by wind. This model will enable us to define optimal design parameters for power generation in any planetary conditions.

2. Design and development of a proof-of-concept inflatable Tumbleweed ball rover generating electrical power with a single-axis pendulum.

3. Demonstration and testing of the concept in the field and providing data to validate the analytical model and quantify power generation capabilities of such a system.

The novel contributions of this work compared to the current state of the art can be summarized as follows:

1. Development of a parametric analytical model for a ball-shaped, wind-blown rover capable of generating electrical power utilizing a pendulum.

2. Development of the pendulum mechanism capable of generating electrical power in a Tumbleweed rover.

The following sections of this document will cover in more detail the prior art relating to ball rovers and more specifically to wind-blown rovers. Afterwards, we will explain the physical background of wind interacting with a ball-shaped vehicle that is impacting its power-generating performance. Furthermore, the thesis will outline some conclusions on the design decisions deduced from the mathematical modelling and will go on to explain the developed proof-of-concept prototype in more detail. In the last two sections of the document the prototype testing and results will be presented, which will validate the mathematical model and provide design consideration for developing a similar vehicle for use on Mars.

Chapter 2

Prior Art

2.1 A brief history of spherical toys and mechanisms

Because the spherical robots and toys provided inspiration to development of Tumbleweed technology, it is necessary to say a few words about early beginnings of movable balls and ball rover technology in general. Although there are numerous patents available related to ball-shaped movable mechanisms, the most important ones are selected and presented herein. These patents date from 1906 to 2008 and all include some kind of a ballast used to achieve propulsion [32]. The first toy vehicles were powered by the spring mechanism with one fixed axis of rotation. The patents present various methods to store and convert that spring energy using different mechanical solutions.

The most relevant patent for this thesis, which is found to use a spherical shape, is coming from the beginning of the century when Benjamin Shorthouse [30] patented a spherical toy (Figure 2.1(a)) that uses a pendulum inside the spherical shell to propel itself. The mechanism also includes a mechanical spring to store the energy for propelling the pendulum and had a capability of manually adjusting the position of the pendulum in order for the ball to move in a desired curved trajectory [32]. A similar mechanical patent came out three years after from Robert E. Cecil [12] who invented a spherical toy

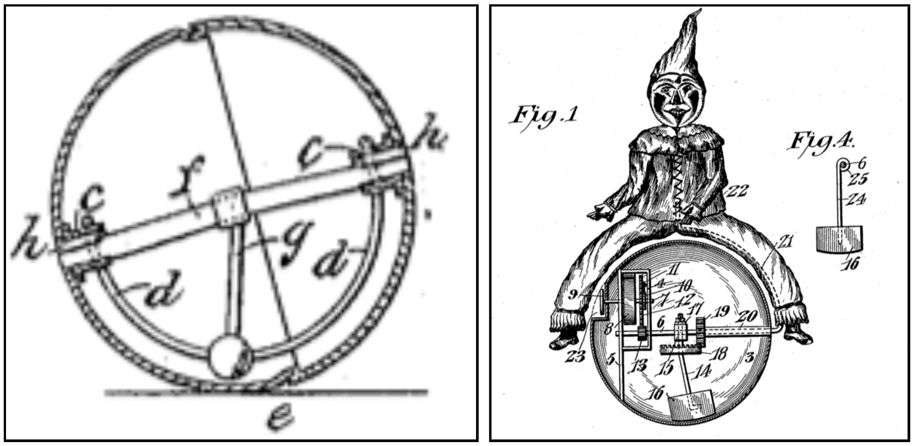

(a) Toy - U.S. Patent 819,609 **(b)** Mechanical Toy - U.S. Patent 933,623

Figure 2.1: First patents relating to pendulum propelled spherical toys. Source: Google Patents, [30, 12]

(Figure 2.1(b)) that moves in a wobbly fashion due to actuation of the pendulum's side movement.

In 1918, Alexander D. McFaul [26] patented a self-propelling toy (Figure 2.2(a)) based on the hamster-wheel concept for propulsion. It also used mechanical spring energy to drive a small hamster-like drivetrain inside the ball. James M. Easterling [14] has invented in 1957 an important addition to self-propelled spherical mechanisms. His device (Figure 2.2(b)) is the first to utilize a battery powered motor that is used to propel the ball with a pendulum. These two patents provide a significant step in the evolution of propulsion of spherical mechanisms and devices.

Afterwards, electric motors were introduced and shock and attitude sensing with mercury switches would control motor operation and rolling direction, as well as adding light and sound effects [32].

In 1974, a motor driven ball with an actuated second degree-of-freedom was patented by Rodger W. McKeehan [27]. The ball had additional mobility capabilities due to that actuated second degree-of-freedom and was able to avoid obstacles by changing direction

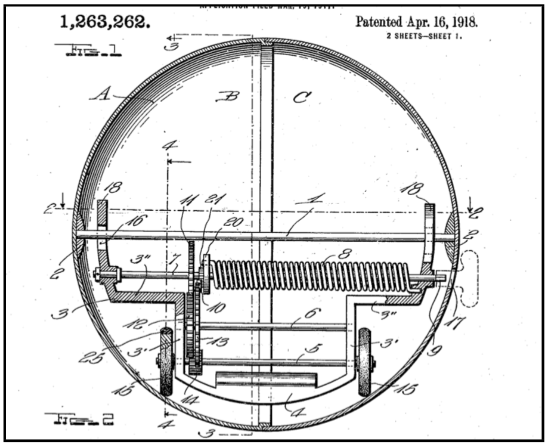

(a) Hamster Ball - U.S. Patent 1,263,262

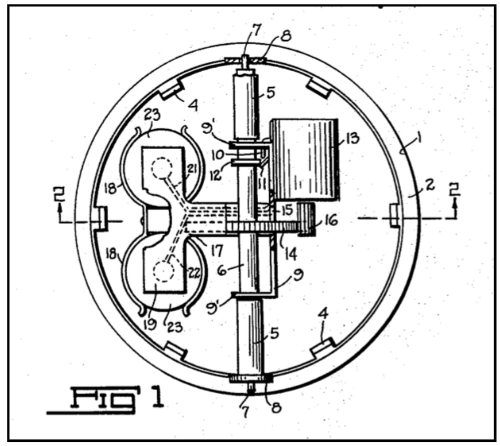

(b) Toy - U.S. Patent 2,949,696

Figure 2.2: Patented ball rover technologies. Source: Google Patents, [26, 14]

while moving (Figure 2.3(a)). Ten years later, in 1985, John E. Martin [24] patented the first radio-controlled spherical device (Figure 2.3(b)) that was moving with the help of a small mechanism with wheels inside the sphere that were remotely actuated.

The most recent inventions include the innovative concepts that shift the centre of gravity of the spherical device instead using the pendulum for propulsion. One such novelty is the Spherical Mobile Robot (Figure 2.3(c)) by Ranjan Mukherjee [28], patented in 2001, that uses several separate weights that are moved with the aid of linear feed systems [32]. Furthermore, Fredrik Bruhn et al. [11] developed a Spherical Mobile Investigator for Planetary Surface (SMIPS) concept that could roll and hop and is based on a Swedish patent held by Per Samuelsson.

It is obvious that many more patents exist that were not covered in this short review, but no prior art was found that addresses the problems of power generation in spherical vehicles. Our concept is the first one that addresses that seemingly marginalized, but important issue.

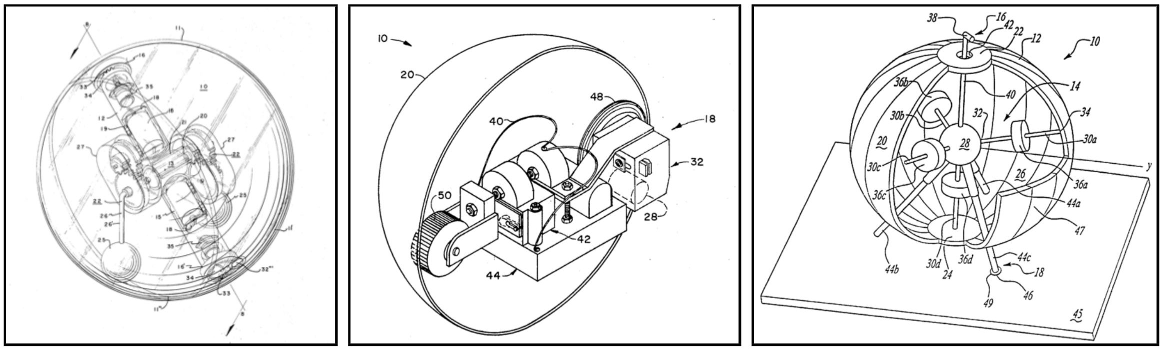

(a) Motor Driven Ball Toy - U.S. Patent 3,798,835 **(b)** Radio Controlled Vehicle Within a Sphere - U.S. Patent 4,541,814 **(c)** Spherical Mobile Robot - U.S. Patent 6,289,263

Figure 2.3: Patented ball rover technologies. Source: Google Patents, [27, 24, 28]

2.2 A history of wind-blown rover development

This following section will focus to describe the history and background of wind-blown Tumbleweed rover technology development at various research institutions. The review will mostly present the works that are more closely related with wind-blown spherical rovers instead of ball rovers in general.

2.2.1 NASA Jet Propulsion Laboratory (JPL), USA

Background

In 1995, Jack Jones of JPL envisioned a large wind-blown ball for Mars that composed of an inflatable structure with a motorized mass hanging below the rolling axis. This would enable driving and steering of the ball while in motion. Driven by the wind, the Tumbleweed ball could cover large distances on the surface of Mars and reach speeds of up to 40 km/h. The tests performed in the 1960s showed that similar inflatable balls could also be used as a landing system because they managed to survive impacts as high as 60 m/s, which was later proven by the deployment of Mars Exploration Rovers and Pathfinder on the surface of Mars with a similar airbag system. This will significantly expand the total mass reserved for science payloads in such rovers [18, 19].

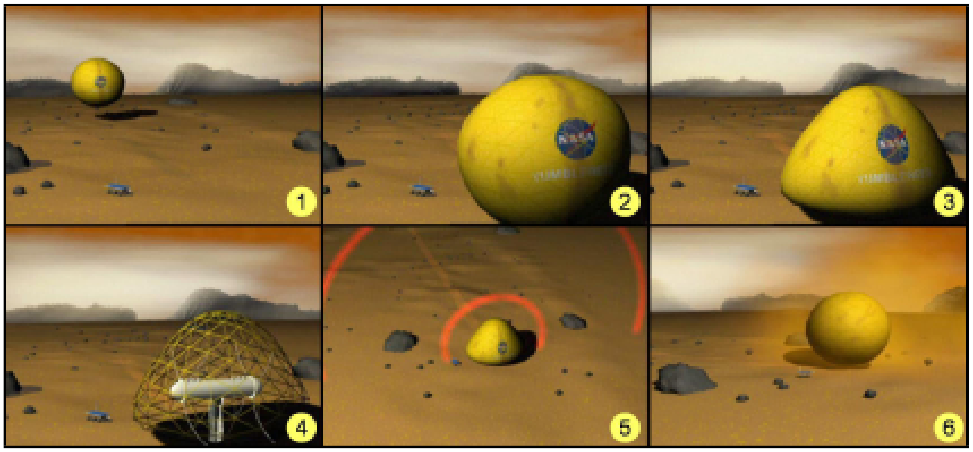

Figure 2.4: Proposed mission scenario for inflatable rover on the surface of Mars - (1) The Tumbleweed Rover is blown around on Mars.; (2-3) Tumbleweed deflates to stop at an area of scientific interests; (4) Instruments are deployed; (5) Data is transmitted to an orbiting satellite network which can relay the data further; (6) Tumbleweed re-inflates and continues its journey. Source: [25]

It was also envisioned that a Tumbleweed could carry internal sensors and science payloads for conducting scientific investigations. Moreover, the inflatable Tumbleweed could be partially deflated to stop at particular locations of interest to take scientific measurements or to reduce its speed [18, 19]. This would be achieved by an internal pump that would be used to re-inflate the ball for continued traversing of the Martian surface. The proposed device would be approximately 6 m in diameter and would weigh approximately 20-40 kg [4, 15].

JPL Tumbleweeds

The first prototype, developed by Jack Jones of JPL, was designed as a 2 m spherical inflatable shell equipped with 3 kg payload suspended by a set of tension cords to keep the payload in the center. The payload included only the required components for successful testing but other instruments (magnetometer, sub-surface water radar, etc.) were planned for integration. In 2002, the same Tumbleweed prototype was equipped with a magnetometer and tested at Arroyo Seco in Pasadena [23].

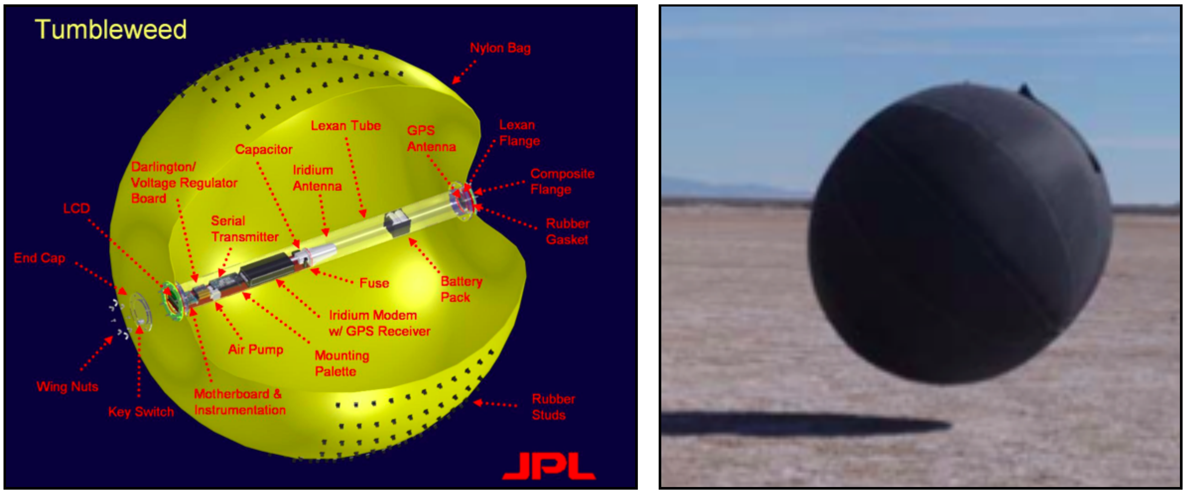

(a) Second generation of JPL's Tumbleweed. Source: [25, 10, 9]

(b) Last generation of JPL's Tumbleweed during the field test in Arizona. Source: [22]

Figure 2.5: Second and third generation of JPL Tumbleweed rovers

Later, Matthews and Behar in collaboration with Jones performed significant improvements in the evolution of the JPL Tumbleweed. Configuration of the second generation JPL Tumbleweed is shown in Figure 2.5(a). The body of the rover consists of a 2 m diameter nylon ball with rubber studs. Rubber studs facilitated rolling along the preferred axis and reduced damage to the shell. A lexan tube is mounted inside the body of the rover along the preferred axis of rotation. The tube is purposely designed shorter in order to prevent the ends of the tube from impacting the ground when the Tumbleweed fails to roll along the intended axis. The lexan tube is attached to the inflatable shell along the whole diameter with a set of flanges and bolts. Rubber gaskets are placed between the flanges to prevent leakage of air [10, 25].

Among other features, this 2 m diameter Tumbleweed rover also had automatic inflation and deflation modes and holds the longest traverse record by a mobile rover (over 200 km in 4 days). The shell of the rover was made out of impregnated Vectran fibres. Furthermore, the electronic package was housed inside the Lexan tube and included: a motherboard with pressure transducers and accelerometers, an Iridium modem with GPS that can provide global telemetry and data collection, and a 900 MHz serial transmitter that enables software upgrade and can transmit measured data and telemetry in the range of 300 m. In addition, a small pump was placed in the tube that enables remote inflation and deflation of the inflatable shell [10, 25].

The third generation of JPL Tumbleweed was developed in 2005 and was successfully tested in 2006 at Wilcox Playa, Arizona. This third prototype is based on previous JPL prototypes with much improved shell and payload integration. The shell in the new prototype is made out of ballistic nylon and kevlar with a diameter of 1.83 m and a mass of 7.25 kg. A cylinder with rover electronics and instrumentation was suspended on a set of cords with a total weight of about 15.4 kg [22].

Preliminary mobility testing

JPL also conducted analysis of aerodynamic and dynamic characteristics of Tumbleweeds in collaboration with the University of Southern California and Carnegie Mellon University. The primary purpose of CMU's test (see Figure 2.6) was to characterize the rolling resistance, drive torque, drive power and tire wear of a single inflatable sphere, for use on the three-wheeled rover, developed by Jack Jones, which utilized the inflatable balls for wheels. [4].

This analysis showed that a 6 m diameter, 20 kg inflatable Tumbleweed was capable of climbing up hills with up to a 20° incline and over 1 m high rocks in Martian winds of 20 m/s [4].

JPL Field Tests

JPL team, have conducted several field tests in the Mojave Desert, California, Pt. Barrow, Alaska, and a long distance test with an instrument payload and satellite communications was conducted in Greenland and Antarctica. In the Greenland field test, a

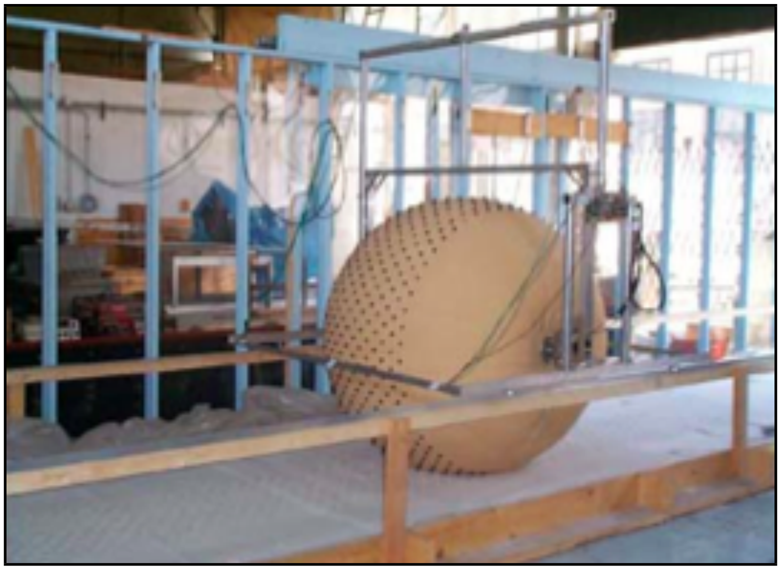

Figure 2.6: CMU Tumbleweed testing facility. Source: [4]

Tumbleweed prototype travelled over 130 km in less than 48 hours. During that time, the rover was sending telemetry and position data to a ground station located at JPL every 30 minutes. Because of the low winds, the rover stopped moving after two days, but continued to send instrument data for nearly 10 days.

Another Tumbleweed deployment was conducted in Antarctica with the objective of reaching the Antarctic coast more than 2000 km away from the South Pole station starting point [10]. After 19 hours and 45 minutes, the inflatable Tumbleweed came to rest some 131 km from its release point and did not to move again for the duration of the test. It is believed that it ceased to move due to lower wind speeds [10]. In this field deployment, the Tumbleweed reached a maximum speed of 17 km/h and averaged roughly 7 km/h. The wind speed at the time of deployment was 28 km/h (15 knots), which propelled the Tumbleweed at roughly 6 km/h [10].

Among other features, JPL's Tumbleweed also recorded temperature and internal and external pressure during this deployment. The Tumbleweed's onboard software activates a pump located in the central tube when the internal pressure drops below a critical level for a specified period of time [10].

In three polar field trials, JPL Tumbleweed traversed 465 km in 24 hours. In August 2003 Greenland test it covered 131 km in 9 days. During a subsequent test near South Pole in Antarctic in January 2004 it traversed 134 km in 7 days. Soon after, in May 2004 on Greenland it traversed 200 km in 7 days [10, 22].

In February 2006, JPL team successfully tested the third generation JPL Tumbleweed in Wilcox Playa, Arizona [22]. The main objective of this field trial was to investigate mobility performance and the effect of boundary atmospheric layer on the Tumbleweed. Video and GPS data were recorded, with meteorological stations deployed close enough to correlate motion with the wind. In that test, the team also performed an experiment by using a surface-mounted flexible solar cells, in order to define the impact of dust and abrasion of the solar cells on the efficiency of power generation. In their experiment a thin-film solar cell is mounted on the outside of the spherical, polyvinyl-chloride (PVC) shell and was pushed around. The conditions of the cells were evaluated after each traverse of up to 300 m. In each test, the cells became dusty, but the level of dustiness did not increase on larger traverses. It was concluded that the dust removal by abrasion overcomes the dust accumulation.

This concept demonstrated that power can be generated with solar cells, but it does not address the issue of solar cell exposure to damage while rolling [22, 21]. Obviously, this effect poses a great reliability concern because during rolling the ball would hit hard obstacles and the frictional abrasion due to ball - ground interaction would be significant. Due to that fact, such concept of power generation in inflatable Tumbleweed rover would not be a feasible solution in any planetary exploration application.

The work by F. Bruhn et. al [11], suggests that the wear of the solar cells mounted on the outside of the shell could be significantly reduced if the cells are covered in hard plastic or just recessed from the surface. In inflatable shells this can be done by adding runner treads abound the inflatable shell, which would add additional complexity to the design, but could also improve the tolerance of the shell to damage.

2.2.2 NASA Langley Research Center, (LaRC

Background

NASA LaRC has developed several concepts of deployable open-structure Tumbleweeds, for the purpose of providing a durable wind-driven vehicle with superior aerodynamic properties and open access to the Martian environment for scientific payloads. Four primary concepts (*Box-kite, Dandelion, Eggbeater Dandelion and Tumble-cup*) are depicted in Figure 2.8. An overview of each concept is presented herein.

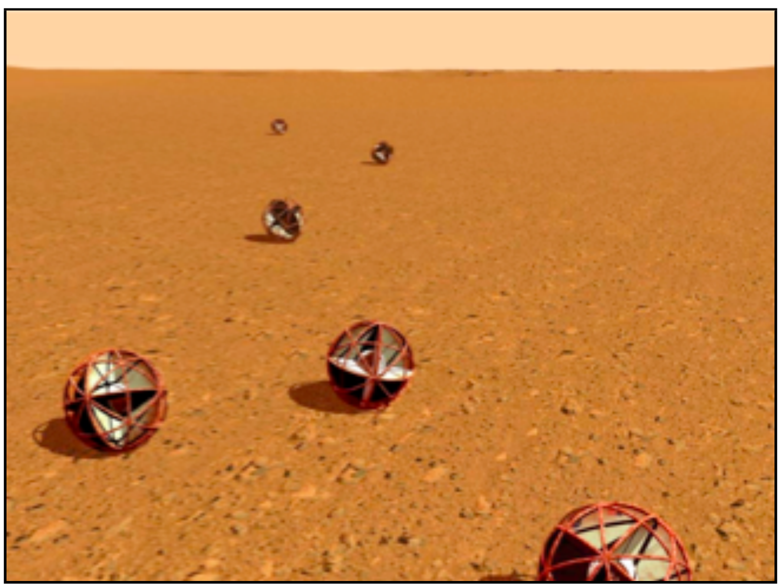

Figure 2.7: LaRC Box-kite mission scenario. Source: [16]

The Box-Kite concept shown in Figure 2.7 is made out of circular hoops with fabric sails. Such design also allows for additional hoops to be included to improve the rolling characteristics of the Box-kite concept [4].

The Dandelion, depicted in Figure 2.9, uses a spherically symmetric array of legs with special convex or concave pads at the ends to prevent sinking into soft surfaces.

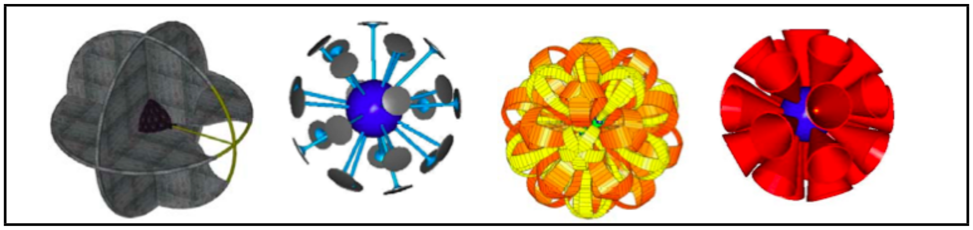

Figure 2.8: NASA LaRC Deployable Open-Structure Tumbleweed Concepts, from left to right: Box Kite, Dandelion, Eggbeater and Tumble-Cup. Source: [4]

A variation of this concept, the Eggbeater Dandelion, consists of multiple curved legs resembling eggbeaters [4].

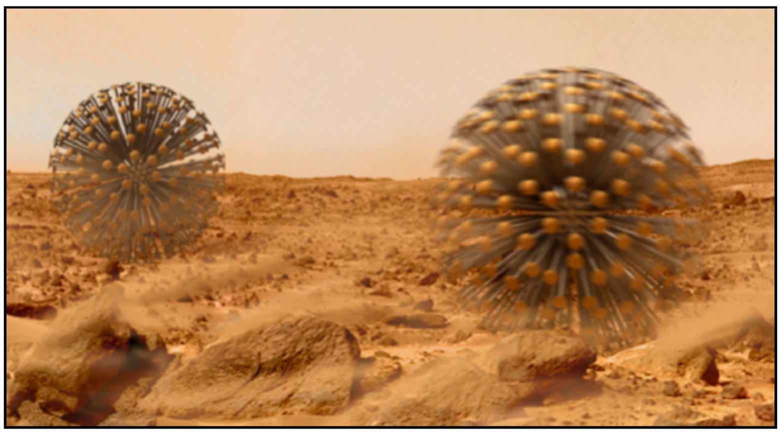

Figure 2.9: NASA LaRC Dandelion Tumbleweed concept depicted on the surface of Mars. Source: [4, 5]

Similar to the Dandelion, the Tumble-cup concept follows the same structural configuration, but instead of the legs, cones or cylinders are used to increase aerodynamic surface area and thus increasing the drag force [7].

The Wedges concept uses inflatable sphere sections to increase the aerodynamic surface and allow for easy payload deployment (Figure 2.10). Instead of using a single inflated sphere, the separate wedge sections are used to form a spherical shape. This could also be a variation of this concept would use small spheres rather than wedges in order to simplify the design). The driving idea behind the Wedges concept is to allow an instrument package to deploy. The Wedges concept would also provide additional durability of the inflatable shell before it collapses by the use of numerous inflated sections [5].

Figure 2.10: NASA LaRC Wedges Tumbleweed concept depicted in the Martian scenario. Source: [5]

In 2007, LaRC was also investigating the feasibility of multi robot control to enable Tumbleweeds to communicate between each other and work together to explore even greater areas than a single unit [31].

Aerodynamic testing and analysis

NASA LaRC performed a very extensive analysis of aerodynamic and dynamic characteristics of Tumbleweed particularly focusing on characterizing the drag of different structural configurations for the purpose of finding a configuration that would increase the air drag coefficient and reduce the size. To properly assess the motion of a Tumbleweed rover in real environments, several analytical models have been developed and many prototype tests conducted to verify assumptions regarding aerodynamic characteristics and rolling properties of the various concepts [4].

Using deployable open structure concepts, the LaRC team wanted to achieve drag coefficients greater than that of a smooth sphere (0.5) in order to minimize the size of

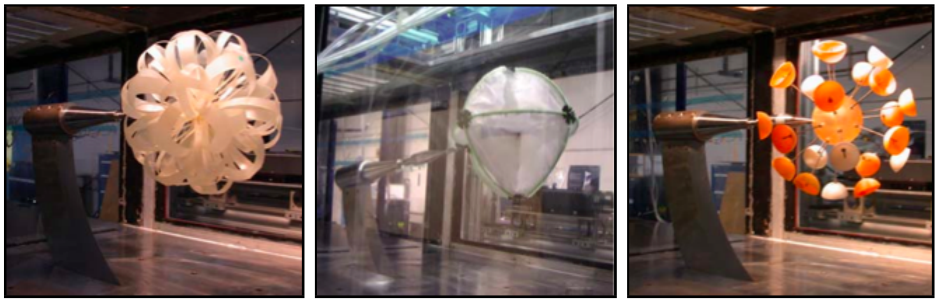

(a) Eggbeater Dandelion **(b)** Box Kite **(c)** Cup-pad Dandelion

Figure 2.11: Evolved LaRC Tumbleweed concepts in BART test section (from right to left, Eggbeater Dandelion, Cloth Sail Box Kite, and Cup-Pad Dandelion. Source: [7]

the Tumbleweed and/or increase the instrument mass capability. Therefore, LaRC has performed a very thorough set of wind tunnel tests to measure the drag characteristics and better understand the Tumbleweed concepts [4, 7].

To precisely simulate the characteristic wind conditions Tumbleweed might be in on the Martian surface, small scale models of 0.3 m with different structural configurations were developed for these tests (Figure 2.11). The first two scaled models were based on the Dandelion concept (Figure 2.11(a) and 2.11(c)), which used legs or struts while the third one was based on the Box-kite idea (Figure 2.11(b)) that used fabric sails [7].

Preliminary analysis of the Box-kite data showed that the drag coefficient C_d, varies from 0.8 up to 1.2 depending on the model orientation and angle of attack [4]. Furthermore, the material in use also showed impact on drag C_d. The Box-kite with fabric sail panels demonstrate a higher drag coefficient than the Box-kite made out of wood. It was confirmed that the fabric sails have a very favourable effect on the drag. [7]. The Eggbeater Dandelion models were very consistent with an average drag coefficient C_d of 0.8. The results for the Dandelion with cupped legs were significantly lower than expected, with the C_d ranging from 0.4 to 0.5, which resembles the drag measured on the smooth sphere. The tests concluded that the Box-kite shows the best drag performance of all

(a) NASA LaRC Box kite baseline Tumbleweed concept. Source:[6]

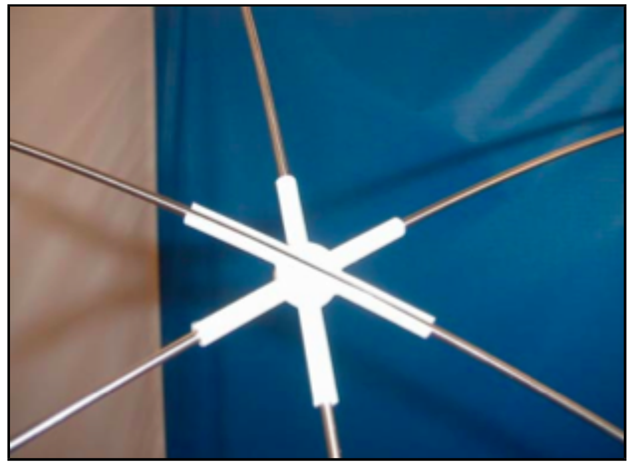

(b) Polycarbonate connecting node used in Box-kite. Source:[6]

Figure 2.12: NASA LaRC Box-kite Tumbleweed rover

tested prototypes. To summarize, the conclusion from these tests is that the Box-kite and the Tumble-cup structural configurations are the most drag efficient with a drag coefficient reaching values higher than 1.

LaRC Box-kite Prototype

NASA Langley Research Center (LaRC) has been studying dynamics, aerodynamics, and mission concepts of Tumbleweed rovers. Based on the preliminary results of NASA LaRC's analyses, the Box-kite concept was selected for prototype development because of its high drag properties, simple design, ease of construction, and open structure for instrument access. The LaRC Box-kite prototype (Figure 2.12(a)) also incorporates knowledge gained from the development of the Tumbleweed Earth Demonstrator (TED), a Box-kite prototype developed in collaboration with the North Carolina State University in 2002/2003 [6].

The LaRC Box-kite Tumbleweed prototype is constructed using 914 mm long sections of 3.175 mm diameter titanium wire (6Al 4 V ELI), joined by polycarbonate connectors

(Figure 2.12(b)) to form hoops. The sails are fastened to the hoops with Velcro and are made from rip-stop nylon sail material. Additional hoops were added between the sail quadrants to facilitate rolling [6]. The 254 mm diameter instrument/payload core, which is located in the center of the vehicle, houses electronics and instruments (thermocouples, pressure sensors, GPS, RCATS). RCATS (Radio Controlled Aircraft Telemetry System) kit was originally designed for unmanned aerial vehicles (UAVs). The total weight of the prototype, including the structure, sails, sensors, and payload core was around 6 kg.

Preliminary field testing of the Tumbleweed prototype was conducted at the NASA LaRC in May 2005. Wind speed measurements showed that the rover achieved mobility in 6-8 km/h winds, despite the soft structure that resulted in a larger footprint and hence more rolling resistance [6]. Additional testing was performed in cooperation with NCSU who developed the Tumbleweed Earth Demonstrator. The NCSU Tumbleweed concepts are based on the Box-kite concept developed by NASA LaRC and depicted in Figure 2.13(a). The outer structure of the TED2 was 3 meters in diameter and was made up of a 5 cm carbon fibre/Kevlar hybrid sleeve. The structure was composed of 24 main members, 2 hubs, and 1 center ring [13]. Inner structure comprised of a gimballed mechanism, which allows the Modular Instrument System (MIS) to remain upright at all times, even while TED2 is rolling.

NCSU also preformed experiments by using solar cells to generate electrical power. In their first experiment, they used flexible solar cells, installed on the box-kite panels (see Figure 2.13(b)) and analyzed the effects of rolling on power generation [4]. Their experiment concluded that a few watts of power can be produced. In their later development, they placed a solar cell array on the top of the MIS housing, which maintained the surface upright even while rolling, and enabling the solar cells to be exposed at all times. However, this solar cell power generation approach does not apply to inflatable shells because the system would have to be enclosed within the shell. A durable, transparent,

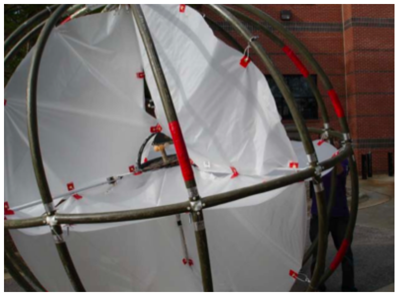

(a) Tumbleweed Earth Demonstrator. Source: [6, 13]

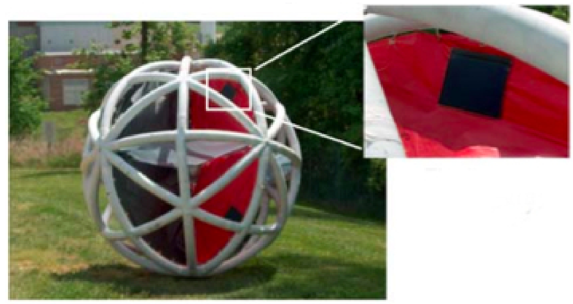

(b) Tumbleweed Earth Demonstrator with solar cells integrated on the side panels of the box-kite like TED rover. Source: [4]

Figure 2.13: NCSU Tumbleweed prototypes

and inflatable shell does not currently exist.

2.2.3 Helsinki University of Technology, Finland

A 1.3 m diameter Tumbleweed prototype (see Figure 2.14) developed at Helsinki University of Technology was equipped with a 2 degree-of-freedom drive system that provided fully steered and motorized locomotion and guidance by using a pendulum [32]. The prototype did not include any power generation equipment, but it is interesting due to its pendulum mechanism. The pendulum mechanism enabled the ball to successfully traverse obstacles of 4.3 cm. Due to its open structure that significantly reduces the drag coefficient, a terrestrial 5 m/s wind is supposed to propel the roughly 4 kg prototype over 10 cm high obstacles [32, 17].

Driving tests showed that locomotion is quite clumsy and chaotic and if the pendulum is steered while the ball is in motion it makes the ball follow a spiral path in which the radius of curvature decreases towards the end of the motion [32]. In practice, it is possible to make the Tumbleweed turn in a very limited space, but controlling the length of the turn is more difficult [32, 17].

Figure 2.14: Helsinki University Technology Thistle rover. Source: [32, 17]

2.3 Conclusions of prior art assessment

In the previous section it can be noticed that a very small number of Tumbleweed technology studies (please refer to [4, 22, 21]) have addressed the problem of power generation in wind-blown spherical robotic vehicles. Moreover, it can also be concluded that solar cells, as a method for power generation, is unreliable and difficult to implement in spherical vehicles primarily because of their unique structural configuration [11]. Therefore, the proposed solution in this work is unique, robust, and solves the problem of power sustainability, thus extending the autonomy of such vehicles and their science capabilities.

Chapter 3

Problem analysis and system modelling

3.1 Problem to be Addressed

In the previous sections we have overviewed all kinds of Tumbleweed rovers. However, a crucial question on how to address continuous power generation in a spherical rover was still left unanswered, which, if addressed, would mean greater autonomy and improved planetary exploration capabilities.

As discussed, some research efforts have been focused on the problem of power generation by flexible solar cells, which were proven not to be a reliable and power efficient solution for spherical rovers [4, 22, 21]. Our proposed solution addressees the power generation problem from a completely different perspective by using Tumbleweed's kinetic energy in order to generate power, which can then be stored in a battery or similar energy storage device and used when needed to either move, guide the robot while rolling, or perform science experiments.

Therefore, developing such a system will build understanding and help to establish design parameters that will guide us to maximize performance of the power-generation capabilities.

3.2 Solution

Our solution encompasses a pendulum mechanism that scavenges the Tumbleweed's kinetic energy to generate electrical power through a generator. Such a robust solution minimizes the complexity of the power generation system and also allows for use of the pendulum to propel the vehicle regardless of the current wind conditions. Furthermore, the pendulum is protected within the spherical shell, which improves the reliability of the system and has unique benefits in operation in foreign planetary environments.

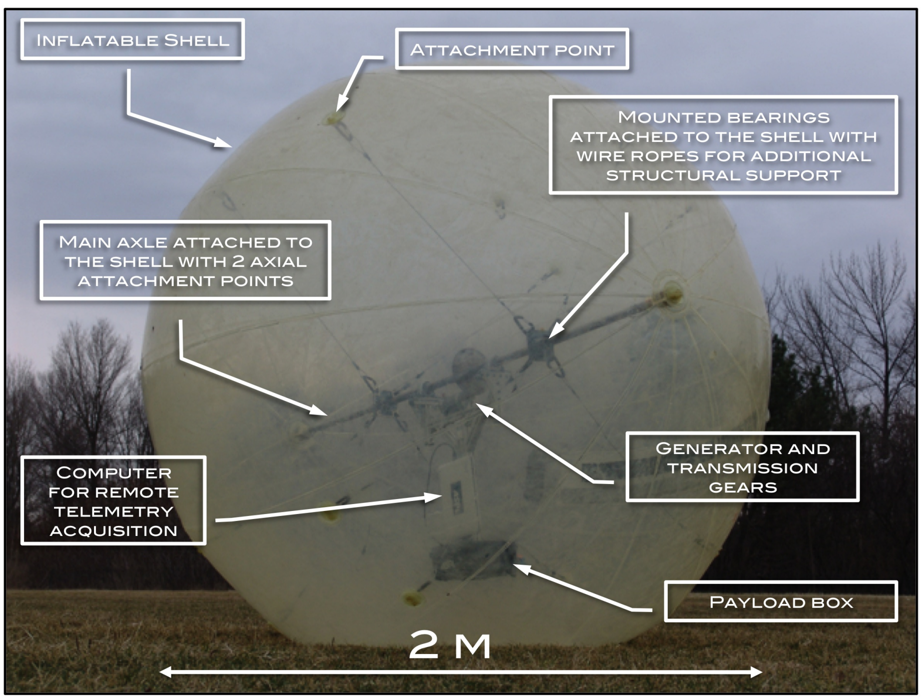

Figure 3.1: 2 m in diameter Tumbleweed Power Scavenging Rover developed in UTIAS ASRL lab

The concept of power generation in this case resembles a windmill mechanism. While the rover is being wind-propelled the pendulum inside rotates around the preferred axis. A DC motor/generator is attached to the pendulum and due to the pendulum's rotation around the main axle, the power is generated. We also used a spur gear in order to maximize the power output and speed up the generator shaft. Our solution also encompasses an electrical load circuit that consists of a load and a rectifier bridge to enable the pendulum to rotate in either direction.

The following parametric analytical model will demonstrate the feasibility of the proposed system and will provide us with an estimate of the power generation capability depending on the design parameters we choose.

3.3 Parametric Analytical Model

A parametric analytical system model was developed that will help predict Tumbleweed performance and make it easier to select key design decisions and fine tune for operation in any planetary environment.

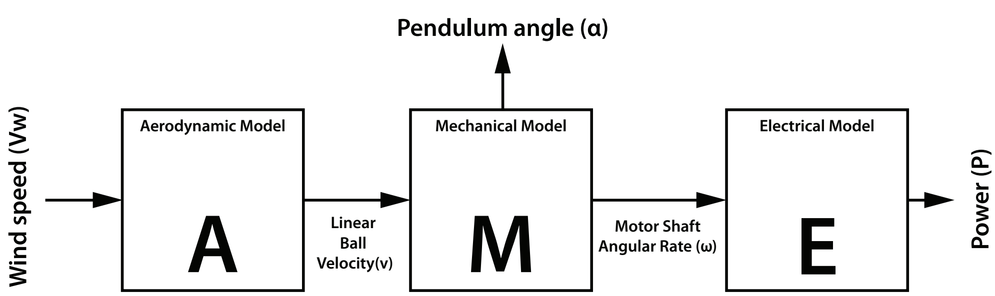

Figure 3.2: Block diagram of the parametric analytical model. The model consists of three sub-models, which describe the process of energy conversion. Aerodynamic model (A) describes the impact of the wind force on the ball. The mechanical model (M) focuses more on the mechanical aspect of the process where the rotation of the ball is being transferred to the shaft of the generator. At the end of the process is the electrical model (E), which governs the final power conversion.

The model consists of three sub-models, which describe the process of energy conversion (see Figure 3.2). First, to successfully generate power and be able to quantify it, we need to understand how current, voltage and resistance are interrelated and how electrical power is produced in the generator. These relationships are presented in the electrical model (E). The mechanical model (M) focuses more on the mechanical aspect of the process where the rotation of the ball is being transferred to the shaft of the generator through gears and other mechanical components. Furthermore, in aerodynamic model (A) we will describe in detail how wind interacts with the spherical body such as a Tumbleweed ball and what impact this has on the power generation capability of such a system.

3.3.1 Initial assumptions and system parameters

Before we proceed, it is necessary to establish system parameters, states, rules, constraints and other system definitions. To do this, we need to establish some basic assumptions:

1. The model environment is quasi-static and represented in a two-dimensions.
2. The Tumbleweed rover is a non-deformable spherical body rolling on a smooth flat surface.
3. The Tumbleweed rover does not slip and remains in constant contact with ground.

System state definition

To model the system successfully, we must determine the physical variables that describe the system's state. By observing a rolling Tumbleweed rover, it can be noticed that the most important state variable is the angular velocity of the ball because power generation depends on the angular velocity provided to the generator. Another important component required for quantifying power generation is the moment produced on the shaft, which is directly responsible for generating current. Furthermore, it can be observed that the same moment creates the deflection of the pendulum with respect to the gravity gradient and therefore can be used as another state variable.

There could be other state variables defined, although they are not of particular interest to this project. The state variables just described above can be seen summarized in Table 3.1.

State variables	Description	Units
ω	Rotational speed around the main axis	$\frac{\text{rad}}{\text{s}}$
I	Current	A
α	Pendulum angle	rad

Table 3.1: Tumbleweed state variables

Measuring the performance

Based on the goals and objectives of this study, a way of evaluating performance of the Tumbleweed rover has to be established. To fully describe performance of each state the rover can be in, the following variables described in Table 3.2 were taken as prime performance metrics.

Performance Metric	Description	Units
P	Power generated	W
v	Linear velocity of the ball	m/s
α	Pendulum angle (relates to stability)	rad

Table 3.2: Tumbleweed's defined performance metrics

The goal of the performance evaluation is to understand how a combination of different system components influence these performance metrics. Obviously, in our model we will try to establish a set of system components that will provide the maximum power output and as few energy losses as possible. The more power is generated the more it can be used to supply other systems and extend mission life. The linear velocity metric should also be maximized in our calculations primarily due to its tight relationship with power generation in the system and its impact on the Tumbleweed's ability to cover large distances. However, the pendulum angle metric should be kept as minimal as possible because we are trying to avoid the pendulum starting to tip over the axis of rotation, thus not generating any power. The exact method of calculating these variables will be explained in more detail in a later section.

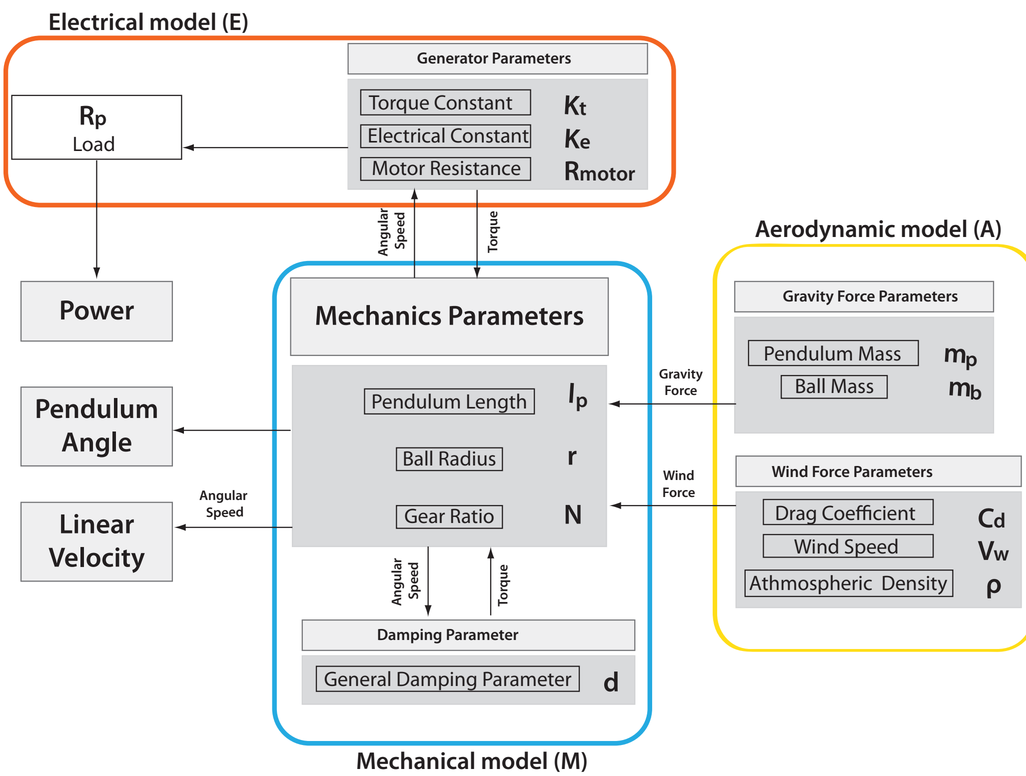

Figure 3.3: Map of parameters impacting the performance of the system.

System parameters

The performance of the power generation capability in this concept greatly depends on the wind and the force it produces on the ball, but it also depends on a set of other parameters that quantify energy losses in the system. Precise definition of these parameters will help us to provide a more accurate estimate on our performance metrics. In Table 3.3 the parameters involved in the system are defined. Some of the parameters presented are design parameters that we can influence with our design decisions, while others are fixed physical parameters or constants. The map of the parameter interaction in the system is given in Figure 3.3.

Parameters	Description	Units	Comments
l_p	Pendulum length	m	-
m_p	Pendulum mass	kg	Pendulum assumed to be a point mass
r	Radius of the inflatable shell	m	Assumed to be a perfect sphere
g	Acceleration due to gravity	$\frac{m}{s^2}$	-
V_w	Wind speed relative to the ground	$\frac{m}{s}$	-
ρ	Atmospheric density	$\frac{kg}{m^3}$	Planetary environment constant
C_d	Drag coefficient	-	Dependent of ball structure and material
A	Frontal area of the sphere	m^2	Cross-sectional area of wind impact
R_{motor}	Motor resistance	Ω	Resistance of the generator's
L	Motor inductance	-	Excluded because of the steady state condition.
K_t	Motor torque constant	$\frac{Nm}{A}$	Motor constant
K_e	Motor voltage constant	$\frac{V}{rads}$	Motor constant
K_v	Motor speed constant	$\frac{rads}{V}$	Motor constant
R_p	Payload resistance	Ω	Load on the circuit
N	Gear ratio	-	-
d	Friction coefficient	$\frac{rad}{Ns}$	Damping due to friction and ball-ground interaction.
$R_{circuit}$	Resistance due to cables and wiring	Ω	Resistance occurring because of the internal wiring
V_{diodes}	Voltage drop occurring due to diodes	V	Voltage drop in the rectifier bridge

Table 3.3: Tumbleweed system parameters

3.3.2 Mathematical representation

In order to maximize the rover's power generation capabilities, the design of the system will be greatly influenced by the parameters mentioned above. A parametric analytical model was created in order to validate and quantify those design parameters and to see what effect on the system will happen when some of these parameters change. This way we can easily understand the impact of environmental variables (wind velocity, air density, drag, etc.) on the system's power-generation capabilities. In this section, the variable relationships and their impact on the system will be explained in detail.

Wind - Ball interaction

While considering the design decisions it was necessary to understand the interaction between the ball, ground, and wind, and what conditions govern the final pendulum power output and other performance metrics defined previously. If we look at the 2D example shown in Figure 3.4 we can see a simple definition of forces and moments involved as the wind force is acting on the ball. In this process the wind applies a non-uniform force to the ball which overcomes the friction resistance occurring on the contact point and providing the ball with some angular momentum. In this model we assume that there is no slipping occurring, which would be highly unlikely in the real world experiment where some slipping could occur.

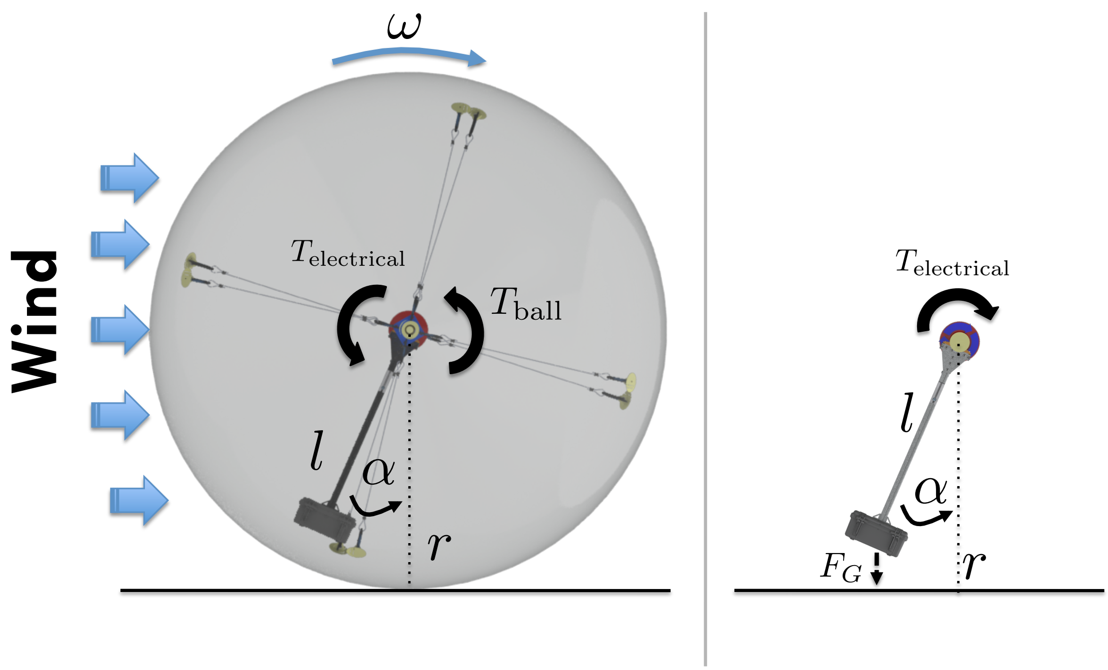

Figure 3.4: Forces and moments acting on the ball and the pendulum.

Because a Tumbleweed rover with a pendulum is a two body system, the energy provided by the wind will be counteracted by two sources thus creating a torque that does work to take energy out of the system. In Figure 3.4 we can see that there are two losses that are occurring. T_{ball} represents the loss that occurs due to interaction and friction between the ground and shell of the ball. $T_{\text{electrical}}$ is a moment that occurs due to the pendulum deflection from the gravity gradient. This system described in mathematical terms is:

$$rF_w = T_{\text{ball}} + T_{\text{electrical}} \tag{3.1}$$

where T_{ball} represents the torque occurring due to rolling resistance, and $T_{\text{electrical}}$ is the torque generated from the electrical generator interacting with the pendulum while the ball is rolling. F_w describes the force produced by the wind on the frontal area of the ball taking into account the air drag and air density. This following relationship can be expressed by:

$$F_w = \frac{1}{2} C_d \rho A \underbrace{(V_w - \rho\omega)}_{\substack{\text{velocity of the object} \\ \text{relative to the wind}}}{}^2 \tag{3.2}$$

while

$$T_{\text{ball}} = d\omega. \tag{3.3}$$

Now that the basic relationships are established in the ball frame, we still have to determine the relationship of the moment occurring on the generator, which is a function of the motor torque constant K_t and current I. We will see later on how current can be described in this model. In order to determine the moment occurring as a result of the generator electrical characteristic, we have to first explore what is happening with the pendulum and how the current generated is related to the torque developed as a result of the ballast aiming to reach a force-balanced state.

We have the following:

$$\underbrace{F_G}_{\text{mg}} \overbrace{l}^{\substack{\text{pendulum}\\ \text{length}}} \sin\alpha = T_{\text{electrical}} \tag{3.4}$$

$$mgl\sin\alpha = \underbrace{N}_{\substack{\text{gear}\\ \text{ratio}}} K_t I \tag{3.5}$$

By establishing the relationship above, it can be seen that the moment that occurs on the generator is a function of the force of the gravity pulling the pendulum point mass, which is in an unbalanced state due to ball rotation. Substituting equation 3.4 into equation 3.5 the following can be deduced:

$$T_{\text{electrical}} = NK_tI \tag{3.6}$$

These two models describe the mechanical model of the Tumbleweed configuration with a pendulum. A detailed analysis on the dynamics of wind-blown spherical two-body system that utilizes pendulum for power generation can be found in [29].

How does generator produce power? - Electrical model

Now that we have understood the background of how the wind impacts the ball and what are the basic physical principles behind it, we must understand how the generator converts kinetic energy into electrical energy. Therefore, a relationship between mechanical energy and electrical energy and its conversion has to be explained in more detail. At first, in order to describe processes in the generator, it has to be clear how this conversion happens. The unique arrangement of magnets and winding in the generator define in detail how well the generator converts the mechanical power (speed and torque) into electrical power (current and voltage) [20].

The general concept of that energy conversion process is depicted in Figure 3.5. The voltage and current are produced in the generator with some losses, mainly due to wind-

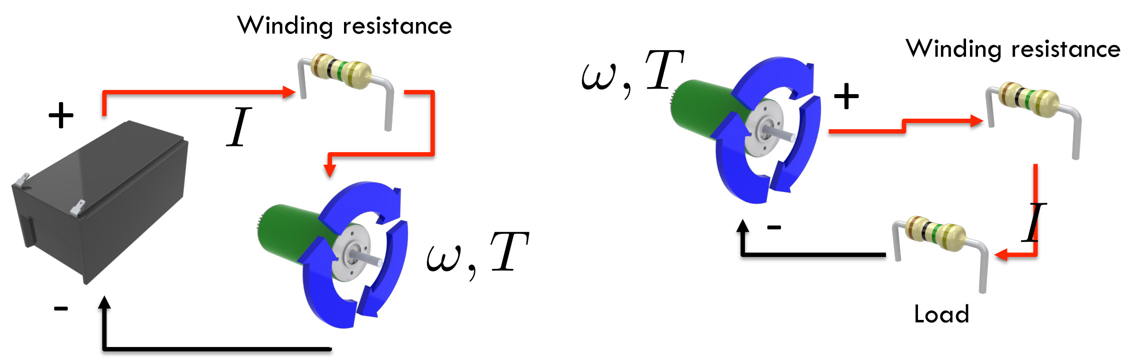

Figure 3.5: Schematics of the general concept behind kinetic to electrical energy conversion.

ing heating, and delivered to the load, which is represented by R_p. Motor inductance, presented by L is also shown but has no relevance in our case since we are evaluating a steady state condition. This relationship is in detail defined by the torque constant, K_t, of the motor, which is usually supplied by the manufacturer where the constant is precisely measured. The speed constant, K_v, is also provided by the manufacturer, but it can also be inferred from K_t because these two constants are very tightly related together. K_v determines how quickly the motor shaft has to turn to generate 1 V. Subsequently, electrical constant or K_e determines how much voltage is needed to make the generator/motor shaft rotates once per minute or to rotate one radian in a second. This can be summarized by the following [20]:

$$\underbrace{K_t}_{\text{(Nm/A)}} \underbrace{K_v}_{\text{(rpm/V)}} = \frac{60}{2\pi} \tag{3.7}$$

This key relationship helps us to deduce further how other constants are interrelated and can be summarized as follows [20]:

$$K_e = \frac{1}{K_v} \tag{3.8}$$

In the Tumbleweed, electrical power will be generated using a pendulum that will rotate around the main axis as the ball is rolling. Because the generator direction of rotation is dependent on wind incidence angle, a rectifier bridge circuit has been designed that maintains the polarity regardless of the generator direction (see Figure 3.6). The mass of the pendulum is pulled by gravity and causes the generator shaft to rotate. The circuit connected to the generator acts as a load and if a battery were connected, it would serve as a charging circuit.

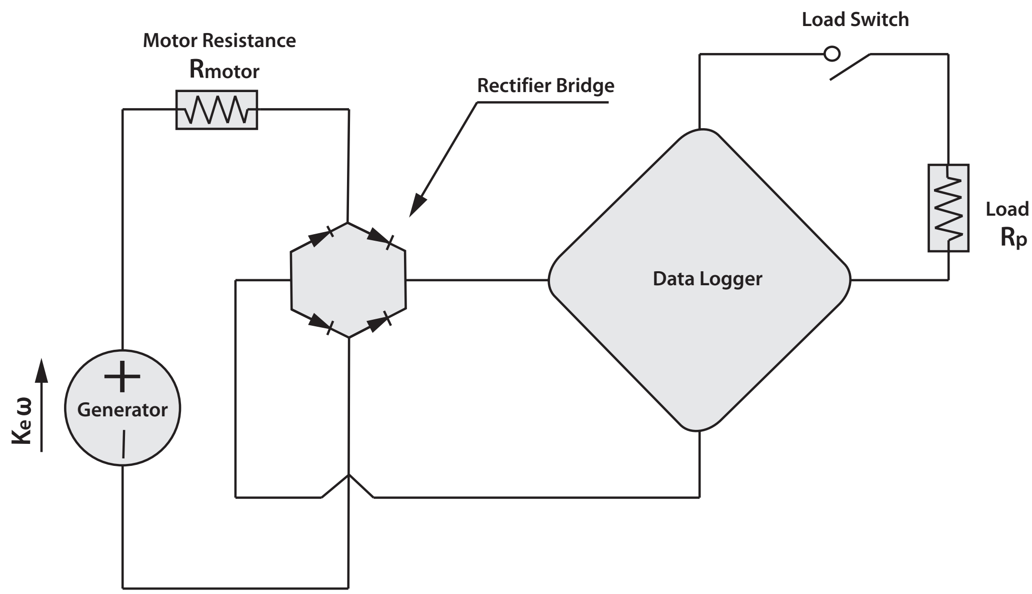

Figure 3.6: Schematic of the load circuit with the rectifier bridge to maintain polarity in any generator rotation direction

Following Kirchhoff's voltage laws, which state that the sum of voltages around any closed circuit must be zero, we can conclude:

$$\sum_{k=1}^{n} V_k = 0 \tag{3.9}$$

The basic principle which makes the generator induce voltage is based on the electric motor conversion equation that states:

$$V = K_e \omega \tag{3.10}$$

The equation above states that the voltage produced in the generator is directly dependant on the motor's electric constant and the speed of rotation of the generator's shaft. In order to apply the same principle in this particular case, we need to define certain losses that occur on the electrical side. To describe such a relationship we need to use Kirchhoff's laws and the fact that the voltage of the generator has to be balanced out with the back electromotive force (EMF) voltage induced at various components in the circuit. Based on these factors, we arrive at the following:

$$NV = V_{\text{motor}} + V_{\text{payload}} + V_{\text{diodes}} + V_{\text{circuit}} \tag{3.11}$$

Following Ohm's law that states $V = RI$, we can substitute some unknown variables that brings us to the following:

$$NV = \underbrace{R_{\text{motor}}}_{\substack{\text{resistance occurring}\\ \text{in the motor winding}}} I + \underbrace{R_{\text{payload}}}_{\text{load}} + \underbrace{R_{\text{circuit}}}_{\substack{\text{resistance of the}\\ \text{circuit components}}} I + V_{\text{diodes}} \tag{3.12}$$

By substituting the equation (3.10) into the equation 3.12 we get

$$NK_e\omega = R_{\text{motor}}I + R_{\text{payload}}I + V_{\text{diodes}} + R_{\text{circuit}}I \tag{3.13}$$

Rearranging (3.13) we can solve for current (I):

$$I = \frac{(NK_e\omega) - V_{\text{diodes}}}{R_{\text{motor}} + R_{\text{payload}} + R_{\text{circuit}}} \tag{3.14}$$

Solving for current, I, provides a definition on how current corresponds to voltage in the load circuit together with all sensors and a load whether this load is a battery or just an equivalent circuit represented by the resistor. Now, all back EMF voltage and resistances can be easily calculated by following Kirchhoff's laws and, likewise, the power delivered to any component.

Now that we have solved for I, we can establish the following balance by substituting equations (3.2), (3.3), (3.6) and (3.14) into (3.1):

$$\frac{1}{2}C_d\rho\pi r^3(V_w - r\omega)^2 = NK_t\left(\frac{(NK_e\omega) - V_{\text{diodes}}}{R_{\text{motor}} + R_{\text{payload}} + R_{\text{circuit}}}\right) + d\omega \tag{3.15}$$

Rearranging (3.15), the following is produced:

$$\left(\frac{1}{2}\rho C_D\pi r^5\right)\omega^2 + \left(-C_D\rho\pi r^4 V_w - d - \frac{N^2K_tK_e}{R_{\text{motor}} + R_{\text{payload}} + R_{\text{circuit}}}\right)\omega + \frac{1}{2}C_D\rho\pi r^3 V_w^2 + \frac{NK_tV_{\text{diodes}}}{R_{\text{motor}} + R_{\text{payload}} + R_{\text{circuit}}} = 0$$

This is a quadratic expression in ω; solving for ω we can establish dependence of ω on the parameters:

$$\begin{aligned}
X &= \left(\frac{N^4K_e^2K_t^2}{R_{\text{motor}}^2 + R_{\text{payload}}^2 + R_{\text{circuit}}^2 + 2(R_{\text{circuit}}R_{\text{motor}} + R_{\text{motor}}R_{\text{payload}} + R_{\text{payload}}R_{\text{circuit}})}\right)\\
Y &= \left(\frac{\rho C_d\pi r^4 V_w N^2K_tK_e + N^2K_tK_e d - \rho C_d\pi r^5 NK_tV_{\text{diodes}}}{R_{\text{motor}} + R_{\text{payload}} + R_{\text{circuit}}} + \rho C_d\pi r^4 V_w d\right)\\
\omega &= \frac{\left(\rho C_d\pi r^4 V_w + d + \left(\frac{N^2K_eK_t}{R+R_p}\right)\right) - \sqrt{d^2 + X + 2Y}}{\rho C_d\pi r^5}
\end{aligned} \tag{3.16}$$

Calculating the angular rate of the ball, ω, from (3.16) allows us to complete the model and calculate final performance metrics. It is important to note that the positive case of the quadratic equation is ignored because it does not adhere to physical laws. Taking into account that particular case would mean that more energy is produced than was put in the system, which would not be possible.

3.3.3 Calculating performance metrics

In order to evaluate the performance of the wind-propelled Tumbleweed and to quantify what power generation capabilities are possible, power delivered to the payload will be calculated as a product of current flowing through the circuit and the load resistor representing the equivalent circuit. Therefore we have

$$P = I^2R_p. \tag{3.17}$$

Subsequently, the linear velocity of the ball can be calculated as

$$v_{\text{linear}} = r\omega. \tag{3.18}$$

Lastly, the deflection angle of the pendulum plays an important factor because we must understand how the angular velocity of the ball and pendulum mass and size are related. This relationship is established by calculating it from the presented model in the following way:

$$\sin\alpha = \frac{NK_tI}{mgl} \tag{3.19}$$

Having the metrics defined, we can now continue to explain how design parameters are selected.

3.3.4 Non-linear rectifier problem

The model presented above presents the impact of the wind on the ball, but it does not satisfy one important criterion, which has to be modelled separately. The problem arises when wind provides a very small force that is just enough to make the ball rotate but it still does not generate enough voltage to overcome the voltage drop that is occurring over the rectifier bridge in the circuit. This means that there is not enough angular velocity on the generator shaft to even start current flowing through the charging/load circuit explained previously.

Compared to the resistors in the circuit that induce voltage linearly with current flowing through the circuit, the rectifiers, due to their non-linearity, actually work in a completely opposite way. Rectifiers as electrical components maintain the same voltage drop with respect to the current flowing by changing their resistance. Because of that effect, they actually do not become active until the drop is satisfied. This effect, that occurs only when the ball is rotating slowly, will have to be modelled a bit differently than the model above, in order for the results of the model to be correct.

If this is to be correctly presented we have to go back to equation (3.1), which states the following:

$$rF_w = T_{\text{ball}} + T_{\text{electrical}}$$

However, the equation above is applicable only when the ball is generating enough voltage to overcome the voltage drop over rectifiers and therefore generate electrical torque that is resisting the ball rotation and therefore incurring losses. Therefore, the impact of the wind in this case should be modelled as described in equation (3.20).

$$rF_w = T_{\text{ball}}. \tag{3.20}$$

Substituting equations (3.2) and (3.3) we get the following:

$$\frac{1}{2}C_d\rho\pi r^3(V_w - r\omega)^2 = d\omega \tag{3.21}$$

This, again, gives us a quadratic expression in ω:

$$\left(\frac{1}{2}\rho C_D\pi r^5\right)\omega^2 + \left(-C_D\rho\pi r^4 V_w - d\right)\omega + \frac{1}{2}C_D\rho\pi r^3 V_w^2 = 0 \tag{3.22}$$

Rearranging and solving the equation above we get the following:

$$\omega_{1,2} = \frac{(\rho C_d\pi r^4 V_w + d) - \sqrt{d^2 + 2\rho C_d\pi r^4 V_w d}}{\rho C_d\pi r^5} \tag{3.23}$$

Once again, the positive case of the quadratic equation is ignored because it would not adhere to laws of physics.

To conclude, when the ball is rolling at such a small angular rate the generator is producing a very small voltage, which does not satisfy the voltage drop around the rectifier bridge. In that case the circuit behaves as an open circuit and is not introducing any energy losses. Therefore, the model takes into consideration both cases, which enables for a more precise estimate in low wind conditions.

3.4 Selecting key design parameters

The established model will give us basic information and help us tune the parameters to maximize vehicle's performance. Obviously some of the first questions that come to mind when thinking about designing such a vehicle are the shell diameter, pendulum length and weight, generator torque and gear reduction (if required). In the following section we will describe the rationale for the design we pursued in developing the proof-of-concept prototype presented herein.

3.4.1 Ball radius selection

Every planetary environment where such a rover can be useful has its own unique atmospheric properties, which will determine the amount of force applied to the ball, causing it to rotate. The ball diameter will have to be sized accordingly so that the ball achieves mobility in the planetary environment as well as to viably generate electrical power.

Parameters	**Units**	**Value**
Average windspeed	m/s	0 - 20
Air density	kg/m^3	1.22
Acceleration due to gravity	m/s^2	9.81
Surface pressure	kPa	101

Table 3.4: Environment variables and constants of Earth's environement

Taking into consideration the parameters imposed by Earth's environment, summarized in Table 3.4, we can calculate and quantify the power output with respect to the ball diameter.

Based on calculations presented in Figure 3.7, which shows the impact of wind speed on generated power, it is clearly shown that for operations on Earth the best size of the ball would be of 1 m in radius. Because of the close relation between the generator shaft speed and power generation, we can observe the same trend (shown in the graph on the bottom) occurring with the generator's shaft speed. We can also see how the power output is highest in the ball with a 2 m in diameter shell. This is also shows generator's dependence on the angular rate of the ball's rotation. The larger the sphere, the slower it will rotate. It has been already shown that the external structure of the

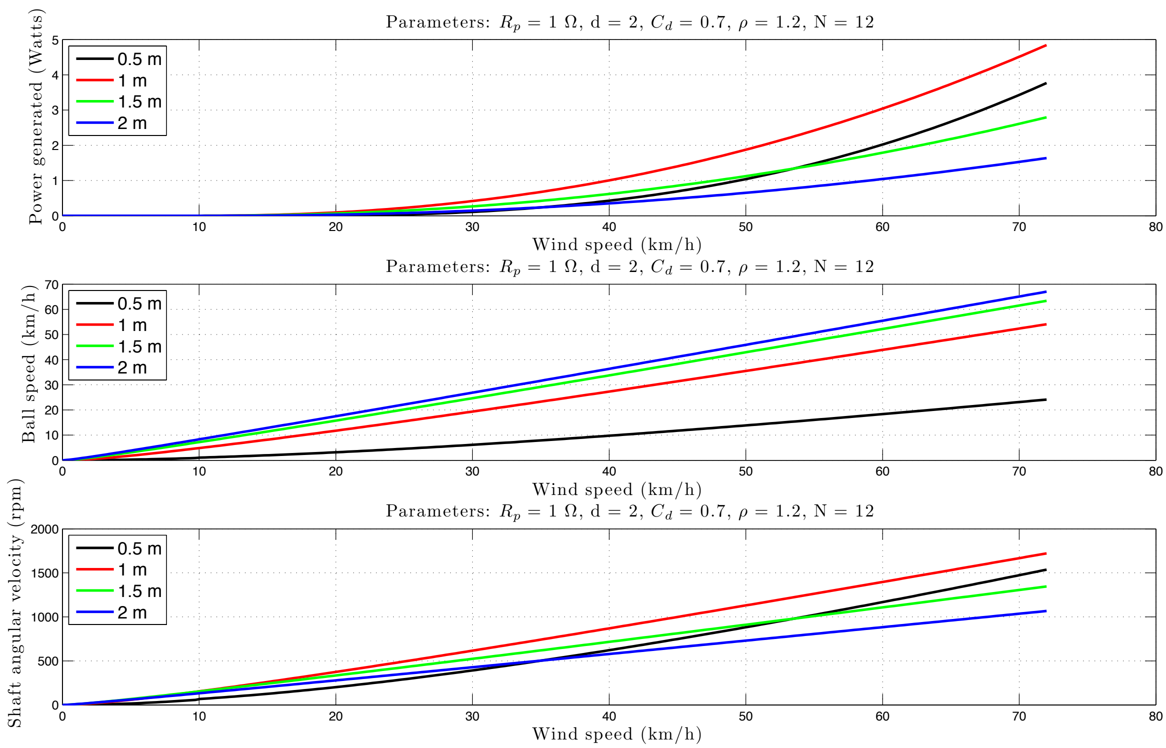

Figure 3.7: Power generated due to wind-ball interaction. Each line in the plot represents different ball radii, while the diagrams show the impact of wind speed to generated power, linear velocity, and the angular speed of the shaft for each of the radius.

ball can significantly impact the drag. Considering the fact that the power generation is maximized when the radius of the ball is 1 m, using an inflatable shell for this prototype was a reasonable solution because it reduced manufacturing complexity and weight of the prototype at a cost of producing a lower drag coefficient.

Also shown in the middle graph is the relationship of various wind speeds on the linear velocity of the ball, which confirms the above mentioned conclusions. The larger the ball is, the more distance will it cover due to larger circumference, but this is inversely proportional to the generated power.

Therefore, based on the model simulation results from the given assumed parameters, we have concluded that the maximum power will be achieved if a shell of 1 m in radius is used.

Parameters	F2260-80W-885	RE 75-250W-118820	RE 40-150W-148867	F2260-80W-880
$K_t(Nm/A)$	0.1	0.0799	0.0302	0.034
$K_v(rpm/V)$	95.4	119	317	278
$R_{\text{motor}}(\Omega)$	1.44	0.181	0.317	0.183
Max. speed (rpm)	4000	4000	12000	4000
Max. winding voltage (V)	24	24	24	15

Table 3.5: DC generator characteristics as listed in the Maxon catalogue

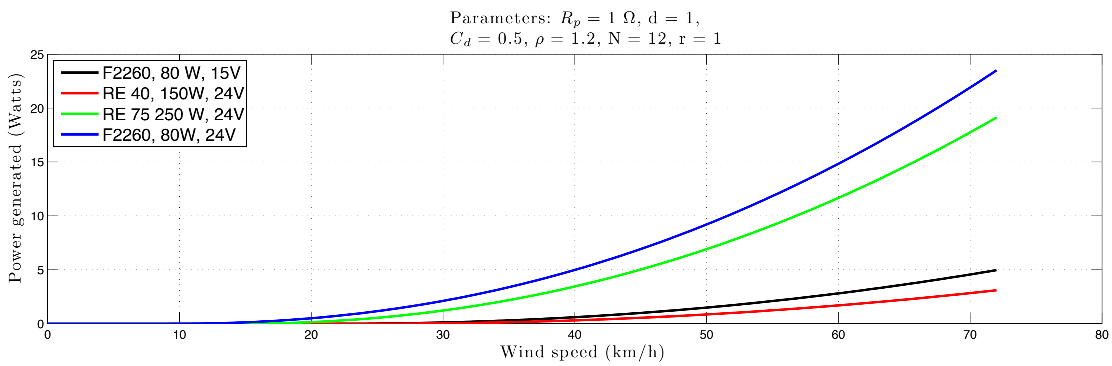

Figure 3.8: Simulated power output of different motors from the Maxon motor catalogue

3.4.2 Generator and gear reduction selection

As we have seen in the previous section, the size of the ball significantly impacts the power generation capability of the system. Selecting a generator that will maximize the power output, was another crucial variable in our design. Therefore, choosing a generator with adequate winding voltage and motor constants can significantly increase the power output. Some additional factors, like winding voltage and highest permissible speed, also have their impact. Four different DC motors/generators were picked from the Maxon catalogue with various characteristics (see Table 3.5).

Observing Figure 3.8, these four generators were compared and we can see the predicted power output for a specific configuration defined in the title of the diagram. The most favourable option would be a generator with largest torque constant, K_t, that does not require high gear ratios and operates anywhere from 10-24 volts. Furthermore, price was also a factor in the generator decision due to limited project budget. Therefore, Maxon F2260-80W-885 was selected as the best candidate for our current application from the available stock.

From the example presented in the bottom of Figure 3.8, we can see that even with a configuration composed of a gear ratio of 12:1, the generator shaft is rotating at a quarter of its permissible speed. A desirable gear reduction would be maximum 18:1, because this would produce a higher angular rate of the shaft at the same wind force and still leave a large enough factor of safety to accommodate even the wind speed of up to 100 km/h without breaching its maximum permissible speed. Based on availability, a gear ratio of 12:1 was selected in order to be able to generate at least 6.5 V and up to 15 W of power.

For the prototype, a direct spur gear mechanism was selected instead of belts or chains. Chains and belts were discarded due to integration complexity and issues that could complicate easy removal of the pendulum from the shell interior. Furthermore, spur gears are also less susceptible to temperature variations or slipping and their cost of integration and additional manufacturing is minimal.

3.4.3 Pendulum length selection

It is desirable to have the mass on the pendulum distributed as low as possible to the ground to achieve the most stability. That will reduce the chance of the pendulum tipping over its own axis and provides additional stability to the ball due to its gyroscopic effects occurring when the ball is rotating at a reasonable speed. If the ballast arm length were very small and close to the center of the ball, the stability of rotation about the preferred axis would be significantly reduced.

In the case of the development of this prototype, we decided that the pendulum length should not exceed 850 mm in order for the payload box to be safely accommodated within the inflatable shell while maintaining a safe clearance to the shell. If the inflatable shell were exchanged for one made of solid material, the pendulum length could be extended a bit more because of much less deformation of the solid shell when rolling compared to the inflatable one.

As we can see in the graphs presented in Figure 3.9, various pendulum lengths are plotted showing how much deflection occurs at various wind speeds. To aid comparison, each diagram presents the behaviour of the pendulum compared to wind speed with respect to the mass of the pendulum. Diagrams show that with our current selection of the pendulum length, the deflection angle in the worst case (smallest mass of the payload box) will not exceed 15°. Furthermore, the diagrams also show that the pendulum angle will reach its maximum position at certain wind speed and will not increase further as wind speed increases. This is occurring because the angle of the pendulum does not depend on the angular speed of the ball, but on the torque happening due to interaction of the pendulum with the axle of rotation. Because the force acting on the ballast is dependant on its mass, the maximum position would increase as the pendulum length and mass decrease.

3.4.4 Load

To generate power and to quantify it, the circuit has to be loaded with a simple resistor circuit or a battery. The diagram in Figure 3.10 presents at which resistance will the system output the most power. We can observe that peak power output is occurring at 2.6 Ω and is maintained across different wind speeds presented in the graph in colours.

Because the peak power output is occurring at such low resistances and is dropping as the load increases, we could say that the best possible way to use such power generation method is to charge a battery due to battery's low internal resistance compared to high-resistance circuits.

In our particular proof-of-concept prototype, we will perform experiments on several different loads ranging from 0-100 Ω.

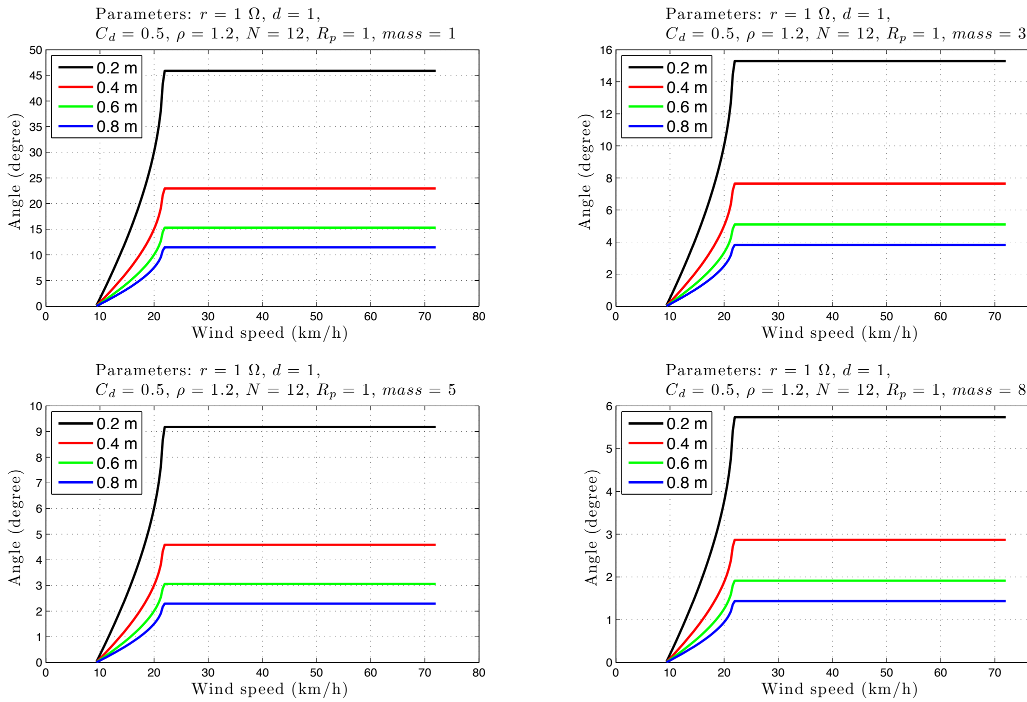

Figure 3.9: Pendulum deflection angle at various lengths. Each plot presents deflection angle occurring with different pendulum weights.

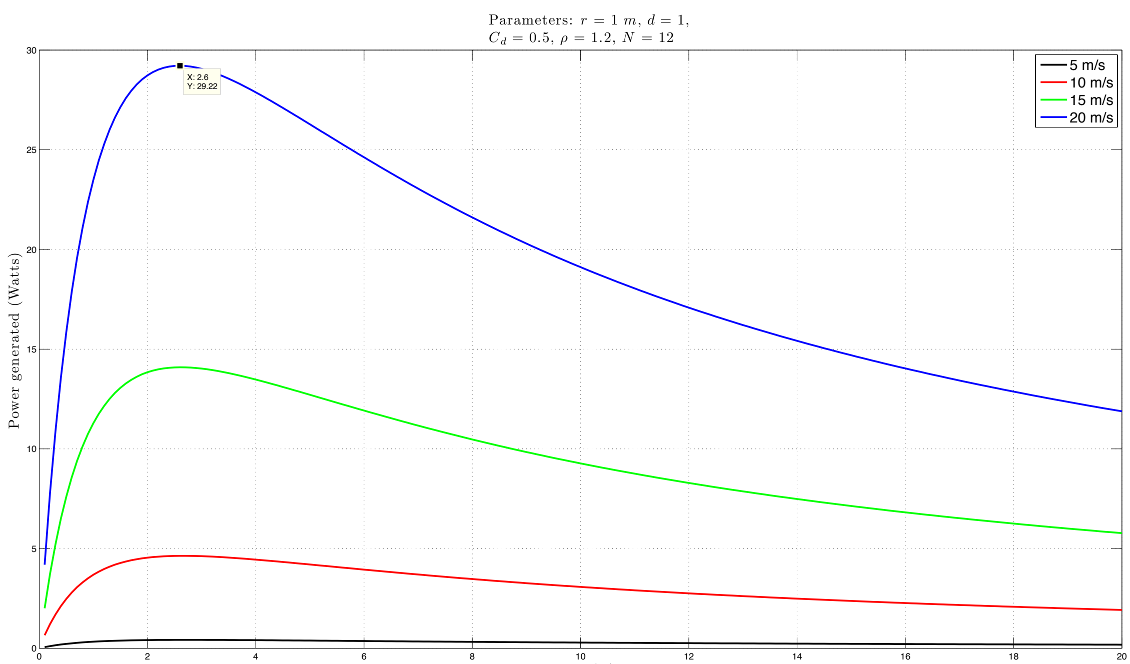

Figure 3.10: Peak power

Chapter 4

System Design and Development

4.1 System Overview

Depicted in Figure 4.1 is the 1 m in radius power-scavenging Tumbleweed rover developed as a part of this thesis. The system was built to prove the concept of power generation in a spherical rover and to facilitate testing and experimenting operations. It is composed of three assemblies:

1. Inflatable shell and supporting structure
2. Pendulum and supporting structure
3. Payload box including the battery for storing the generated power and the data-logging electronics

The system obviously has to be as light as possible and structurally robust enough to endure all mechanical loads on the internal components of the rover. In standard wheeled robot platforms, the main robot platform is located outside its locomotion system while in ball robots the complete structure has to be housed within the wheel of the robot. This provides additional protection of the robot's structural components. However, utilizing an inflatable shell provides several other constraints on power generation and science payload

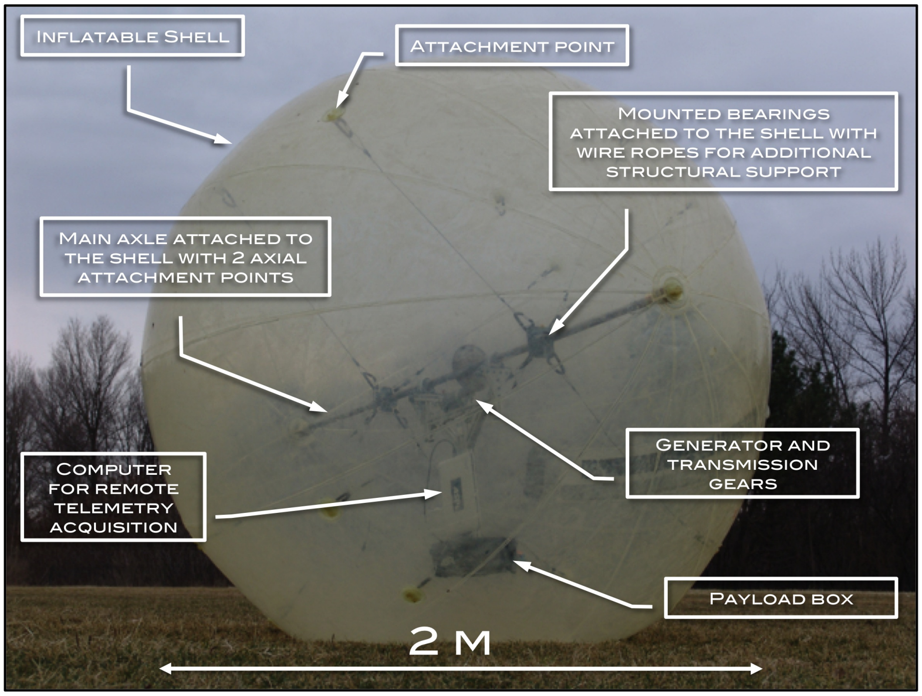

Figure 4.1: Tumbleweed power-scavenging robot

deployment, which are an important factor in rover autonomy and space exploration efforts. The problem of science payload deployment is beyond the scope of this work. Provided in Figure 4.2 is the CAD drawing of the complete system presented without the inflatable shell to increase visibility of all internal components..

A more detailed description of each of the subsystems will be provided in the following sections and Table 4.1 shown below provides a complete mass breakdown of the whole system.

4.1.1 Inflatable shell

The spherical shell, that will protect the internal hardware, is desired to be made out of a high-strength fibre material yet flexible enough to inflate and deflate easily. High-strength

No.	Item description	Product No.	Provided/Manufactured	QTY	Weight/unit (g)
Shell					
1	Attachment point	N/A	Zorb.CN	14	15
2	Inflatable Shell	N/A	Zorb.CN	1	15000
Mechanical					
3	Hollow steel tube	89955K89	McMaster-Carr	1	3128
4	Square mounting bearings	5967K840	McMaster-Carr	2	715
5	U-shaped Mounted Bearings	5913K440	McMaster-Carr	2	345
6	Shims	N/A	McMaster-Carr	10	5
7	Clevis + aluminum inserts	2447K24	McMaster-Carr	2	625
8	Lock pins	98416A-012	McMaster-Carr	2	20
9	Gear 144 with setscrews	A1C2 - N24144	SDP/SI	1	975
10	Gear 12	A1B(C)2 - N24012(A)	SDP/SI	1	3
11	Economy Nuts	N/A	80/20 Inc.	40	5
12	Economy bolts	N/A	80/20 Inc.	40	5
12	1-4/20 screws, HEX head	N/A	80/20 Inc.	4	5
13	Wire rope assembly	N/A	Home Depot	14	25
14	T - connecting plates	25-4112	80/20 Inc.	2	90
15	90deg connection part	25-4132	80/20 Inc.	10	18
18	Extrusion 1010 - 130mm	1010	80/20 Inc.	2	98
19	Extrusion 1010 - 115mm	1010	80/20 Inc.	2	87
20	Extrusion 1010 - 165mm(45 deg)	1010	80/20 Inc.	2	125
21	Extrusion 1020 - 600mm	1020	80/20 Inc.	1	821
22	Extrusion 1010 - 350mm	1010	80/20 Inc.	1	265
23	Plastic Covers	25-2015	80/20 Inc.	6	1
26	Carabiners	N/A	Mountain Equipment Co-Op	14	5
27	Maxon Motor	F2260 - 80W - 885	Electromate Inc.	1	850
28	Maxon Motor shim	N/A	ASRL	2	20
Payload					
29	Payload Housing Pelican 1050	Pelican 1050	Mountain Equipment Co-Op	1	800
30	Circuits	N/A	Home Depot	2	300
31	6 V 3.4 Ah Lead Acid battery	N/A	Digi-Key	1	800
32	eLogger DataLogger (complete)	N/A	EagleTree Systems LLC.	1	180
32	ACER Aspire One Netbook)	N/A	ACER	1	1195
MISC					
29	ZipTies	N/A	N/A	40	1
29	Harness	N/A	N/A	N/A	230
TOTAL					30223

Table 4.1: Tumbleweed system mass breakdown

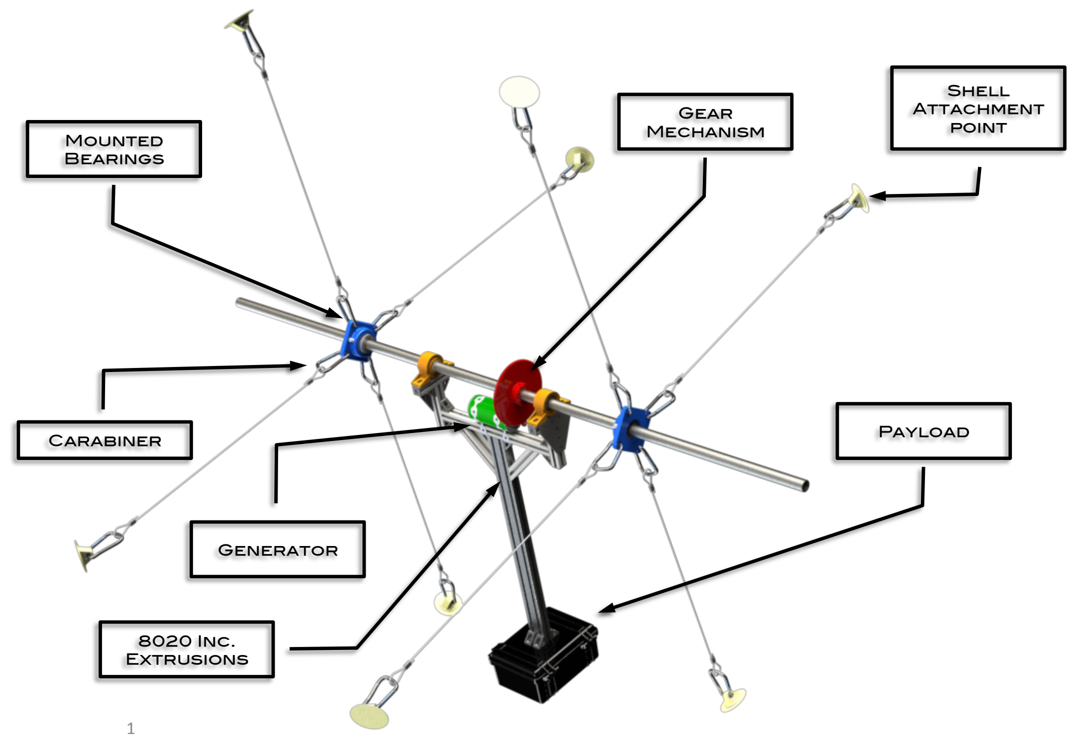

Figure 4.2: CAD drawing of the whole system with all subsystems (inflatable shell not included)

materials like Kevlar, Vectran, or Spectra were considered due to their properties and low wear and tear. After consideration of several manufacturers that provide custom design and manufacturing of high-strength fibres, it was concluded that it would be too expensive to implement in the budget of this project. A more affordable solution was to manufacture the outer shell out of materials such as nylon and TPU (thermoplastic polyurethane).

Another requirement was that the inflatable shell also provide attachment points that are integrated inside the shell and which serve as support for the internal structure of the rover that houses all the electronics, pendulum and the generator. Furthermore, these numerous attachment points will distribute the load imposed on the inflatable shell by the mass of the internal structure. Another important requirement was also that the ball has a zipper to allow for payload integration within the shell. Furthermore, the zipper has to be hermetically closed to prevent the loss of ball pressure.

Considering all these requirements, it was decided that a 1 m in radius shell will be manufactured out of modified beach ball toy that is already commercially available and with affordable cost. The ball is made out of 1 mm thick transparent TPU material and comes equipped with a special rubber zipper for payload integration and an inflation/deflation vent.

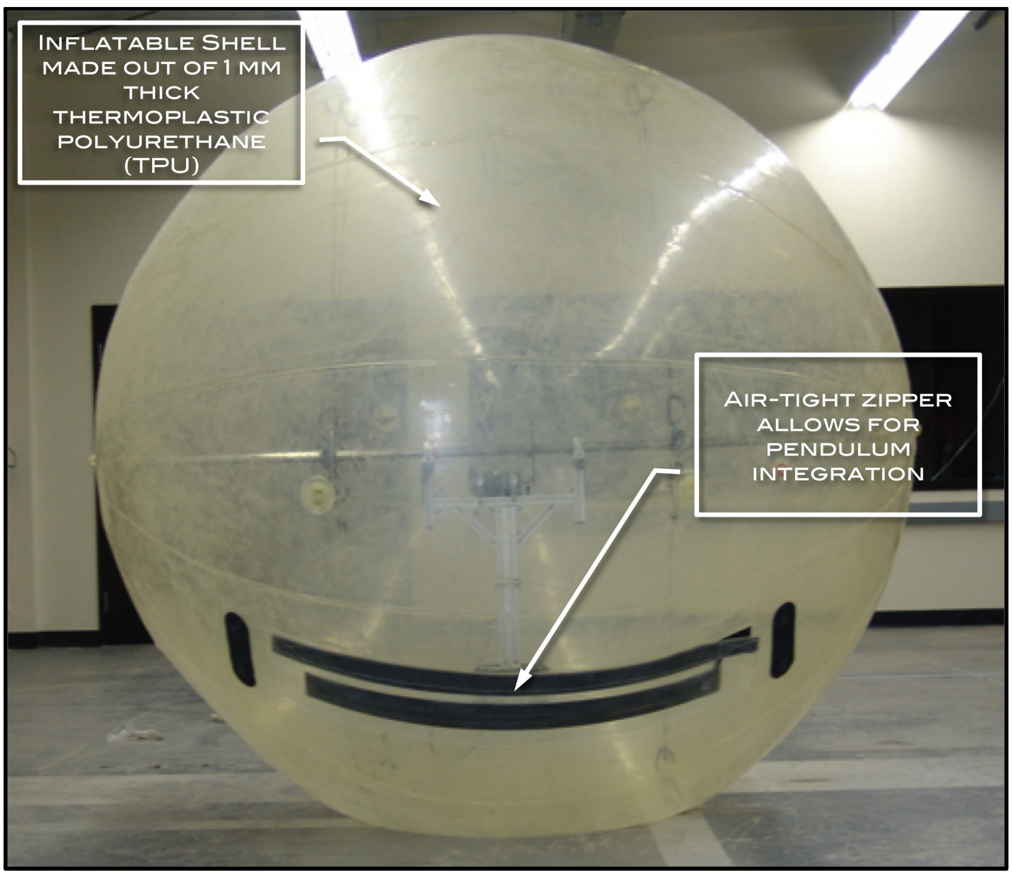

Figure 4.3: TPU shell inflated in UTIAS ASRL lab

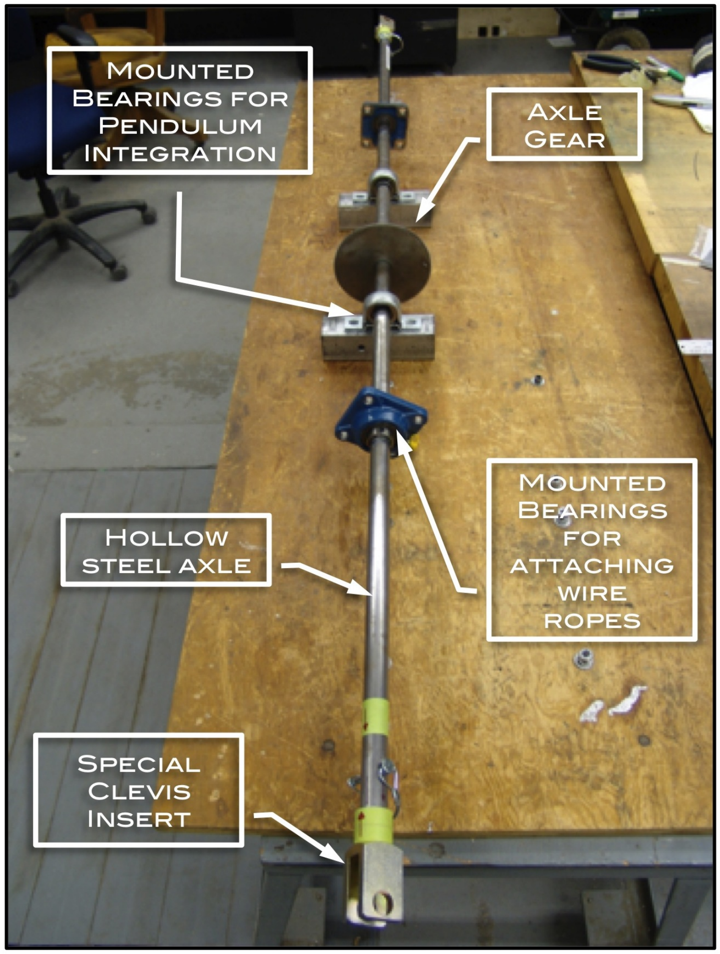

Figure 4.4: Main axle and clevis inserts that are attached to the attachment points on the ball.

4.1.2 Structural components

Main axle

The main axle is the main structural support component of the vehicle since it is diametrically attached to the inflatable shell and provides the support for all mechanical parts of the rover. It is attached between two attachment points of the ball and provides the interface to the pendulum, which rotates around it. The axle had to be made of a very stiff material that would not allow for any bending to occur. Bending of the shaft would create misalignment of the generator gears, which would impact the final performance of the vehicle.

In Figure 4.4 it can be seen how the axle is attached to the clevis inserts, which are then secured to the attachment points inside the ball. Again, the requirement was to find a commercially available hollow rod in order to minimize custom manufacturing and to allow for easy integration with clevis inserts. The design shown in Figure 4.4 allows for complete extraction of the axle if the shell needs to be replaced.

The initial vehicle prototype utilized an aluminum rod that was proven not to be stiff enough and after some tests the axle started to bend under the pendulum load which compromised the gear alignment. Instead, an aircraft steel rod was then selected as the best candidate primarily because of its physical properties.

Support cables and bearings

To prevent the weight of the pendulum and the payload to be solely supported by the two attachment points to which the main axle is connected, an additional 12 attachment points are connected to the main axle via support cables. The support cables are made of aircraft cables cut to length with a loop at each end. The end is then connected to the attachment point via a carabiner on one side and to the mounted bearing secured to the main axle.

The design encompasses two different types of bearings; one provides additional attachment points for support cables and the other one provides attachment interface for the pendulum structure ensuring no misalignment of the gears and minimal motion losses.

This design ensures that the cables can be removed, if needed, allowing removal of the whole main axle component in case the inflatable shell needs to be exchanged. This flexibility of design ensures that any major component inside the rover's inflatable shell can be exchanged without problems, which is a very important feature that increases reliability and autonomy in field operations.

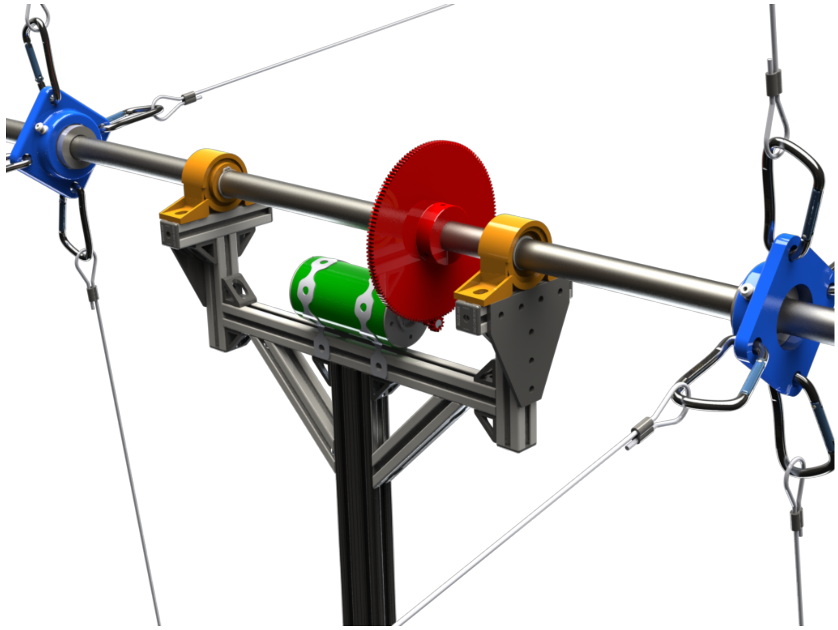

Figure 4.5: Depiction of the support cables attached to the main axle via the mounted bearings

Pendulum

The pendulum structure was assembled out of light components that will allow easy integration with the payload box and the internal structure of the shell. At first, plastic materials were considered in order to achieve lightweight but robust structure. However, the obtained parts would need to be manufactured additionally in order to customize them for this application. To avoid this, the pendulum structure was assembled with 80/20 industrial aluminum extrusions because of the easy integration solution they provide and quite an inexpensive price.

Most important, extrusions did not require any additional manufacturing. One of the main benefits of using extrusions was to allow the pendulum to be easily integrated into the internal support structure of the shell to facilitate extraction and debugging. In Figure 4.7 a final structure can be seen.

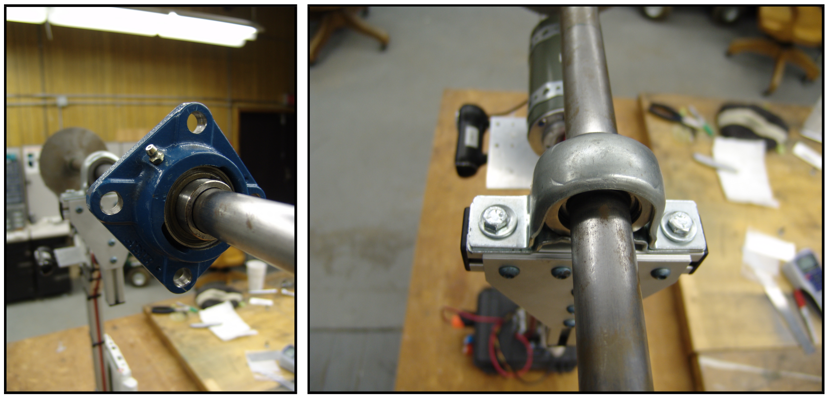

(a) Cast iron mounted bearing

(b) Steel frame mounted bearings

Figure 4.6: Bearings used to provide the interface between the shell, axle and pendulum ensuring equally distributed load while rolling

4.1.3 Mechanical Architecture

DC generator

As discussed in the previous section, Maxon Motor F2260-80-885 W motor was chosen as a generator. In our prototype, the generator is attached to the pendulum structure with two very simple metal straps and some Velcro as shown in Figures 4.8 and 4.7.

Gears

As seen in the previous section on selecting the gear-generator setup, it was advisable that the ratio should be anywhere between 10:1-18:1, which will make sure that the generator rotates well within its predefined permissible speed and to maximize the power output. For the current Maxon Motor F2260-80W-885 motor the highest permissible speed was 4000 rpm equally distributed over 24 V of the winding's highest voltage.

As discussed previously, plain spur gears were selected as the most favourable candidate primarily due to easy integration and availability. The only problem with the spur gears is that they are commercially available only in smaller ratios. Another important

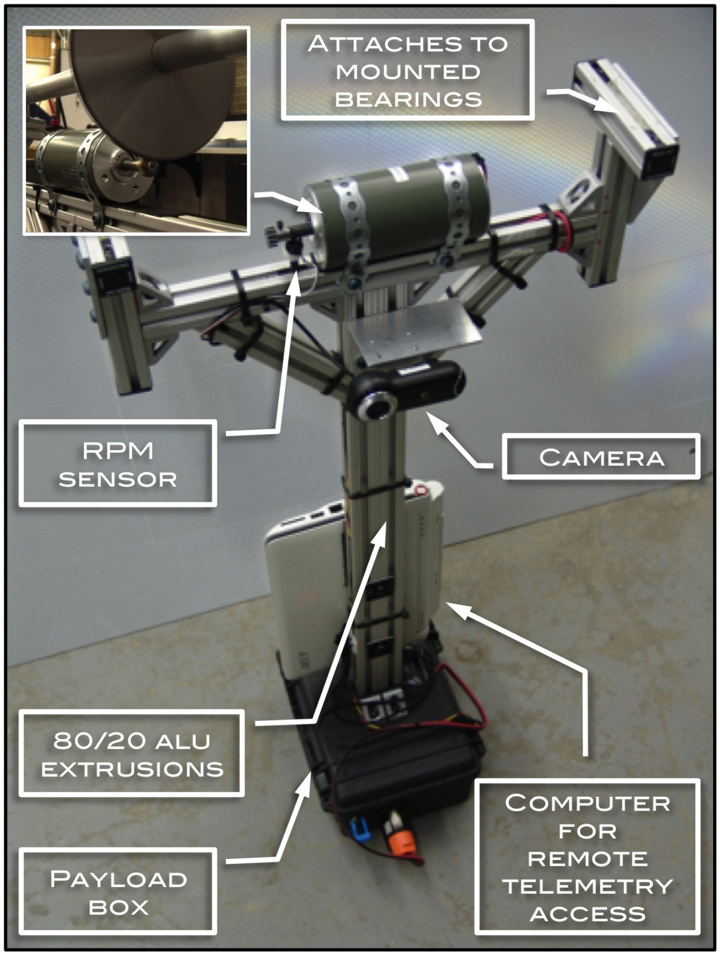

Figure 4.7: Pendulum structure made of 80/20 extrusions with all instruments and components.

constraint was to have gears fit onto the 1" main axle and 6 mm generator shaft.

After considering various manufacturers and gear suppliers in US and Canada the adequate gears were found in SDP/SI Inc. catalogue. The main issue in finding the appropriate gear pairs were the high ratios needed to fit the shaft diameters. Based on all constraints and availability, a gear pair with a ratio of 12:1 was chosen. Please refer to the Figure 4.8.

The 144-tooth carbon-steel gear has a pressure angle of 14.5 % and a diametral pitch of 24. Similarly, a 12-tooth gear had to have the same diametral pitch and pressure angle as the other gear because, otherwise the gears would not match. Small gear was made

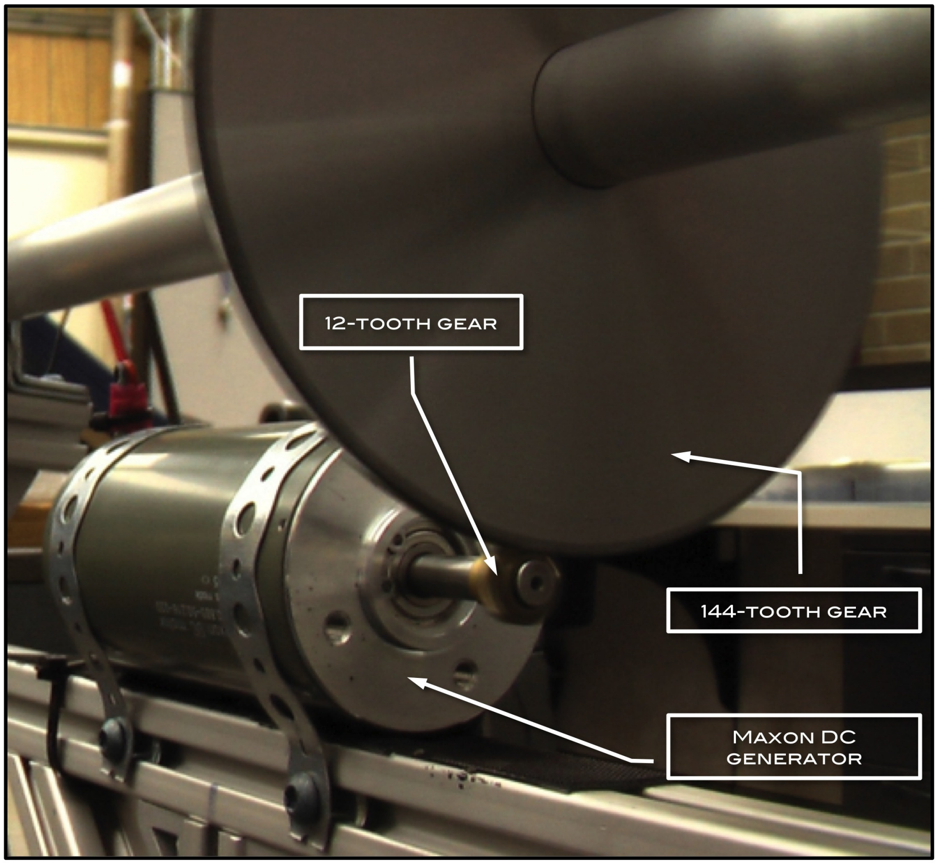

Figure 4.8: Generator with gear reduction assembly.

out of brass, which will reduce wear and tear of the gears during the operation.

4.1.4 Payload

Housing

A Pelican 1120 case was used as a payload housing box. The size of 7.25" x 4.75" x 3.06" (18.4 x 12.1 x 7.8 cm) was perfect for housing of all necessary electronics and sensors needed. Depiction of the arrangement of the electronics and sensory components inside the payload box can be seen in Figure 4.9.

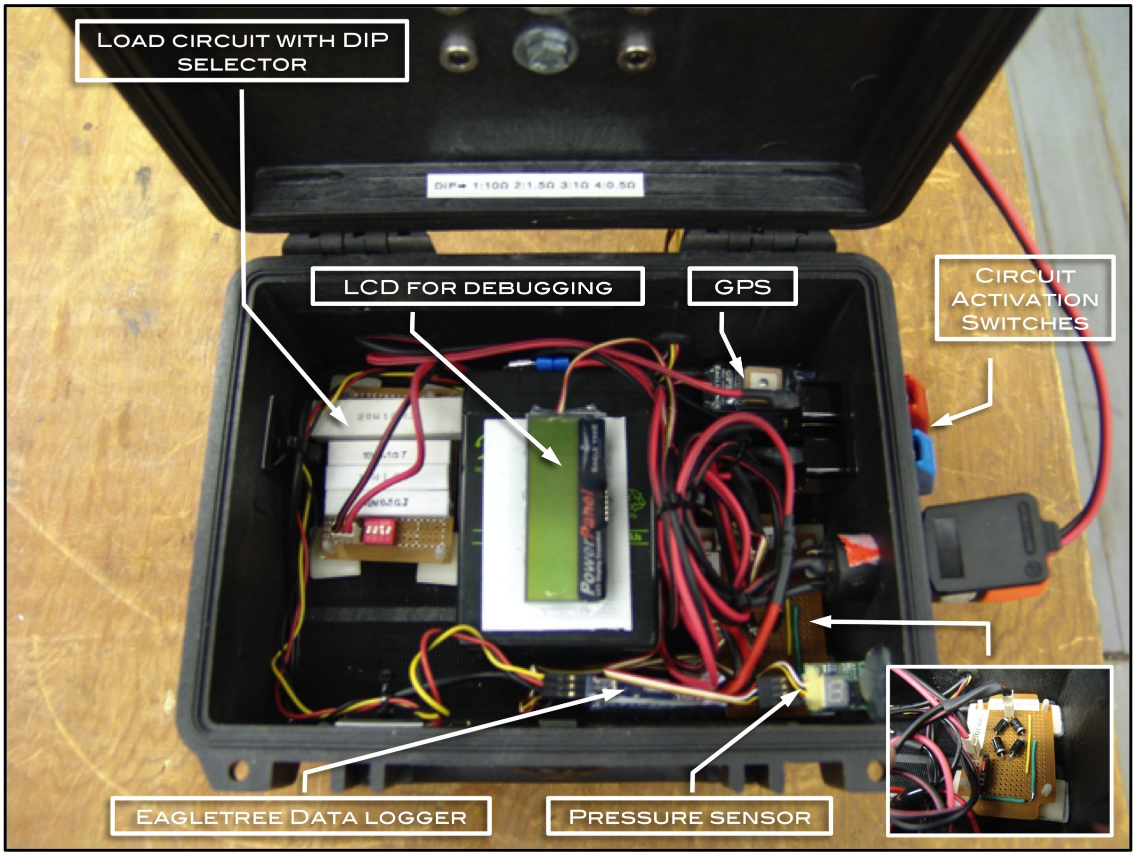

Figure 4.9: Internal arrangement of the electronics and sensors inside the payload box

Rectifier/load circuit

The minimal circuit to generate power will have a load resistor connected in the circuit, to avoid short-circuiting. In this particular case, a minimal circuit also needs to include a rectifier bridge that will maintain the same output polarity in any generator rotation direction and will prevent discharging of the batteries through the motor when not propelled by wind.

The generator is directly connected to the rectifier circuit shown in Figure 4.10(a). The schematics of the rectifier bridge can be found in Figure 3.6. The rectifier circuit is the minimal required power conditioning element to ensure Tumbleweed's safe operation while generating power.

In Figure 4.10(b), a load circuit with resistors can be seen which, is directly connected to the rectifier board. The load circuit consists of several 20W resistors with a selector to allow testing of various load resistances. The load circuit can be disengaged with a simple switch. Figure 3.6 explains in detail the schematics of the electrical system inside the payload box.

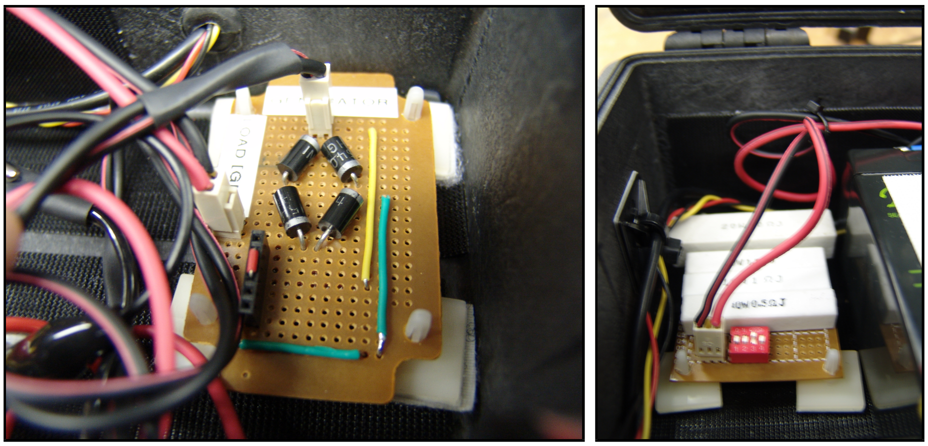

(a) Rectifier circuit **(b)** Load circuit

Figure 4.10: Rectifier and load circuit. Rectifier circuit consists of 4 rectifiers arranged in a bridge to enable power generation in any direction of rolling. Load circuit consist only of resistors and a selector switch for selecting the resistor in use.

Measuring instruments

To obtain telemetry data from the rover in the field operations, a set of sensors and a way to log their output information was mandatory. The main requirement of such a system was high accuracy with a cost within our budget. Furthermore, large memory and a wireless download of the acquired data were also crucial features that enabled smooth field operations and efficient post data processing.

Considering above-mentioned requirements many different data logging systems were found that could satisfy all of the requirements mentioned above. Some state-of-the-art accurate systems, like RCATS or R-DAS, where discarded as potential candidates for

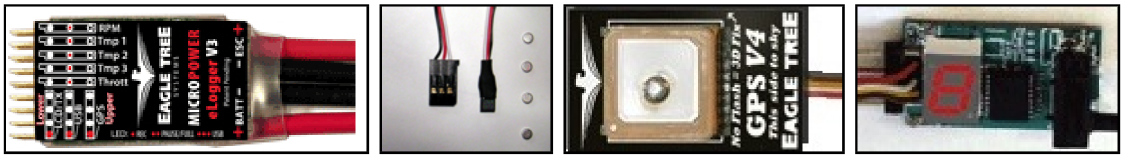

(a) eLogger V3 **(b)** RPM hall sensor **(c)** GPS sensor **(d)** Pressure sensor

Figure 4.11: Data-logging hardware provided by Eagle Tree Systems LLC.

this project primarily due to their expensive price tag. A solution was found in a hobby UAV (Unmanned Aerial Vehicles) industry provided by EagleTree Systems, LLC. Their hardware provided several important features that were easily modified for operation in our testing scenarios:

- up to 70 Volts and 100 Amps data logging
- variable data logging frequency
- live mode for live data monitoring and logging
- GPS logging
- Altimeter which was converted to internal pressure monitoring for this particular application
- RPM data logging and calibration

The hardware was designed to be powered by the battery and measure the motor load on the battery. In this application the load is actually an equivalent circuit or a battery that needs to be charged while the power is supplied by the generator in the circuit. Please see the schematics in Figure 3.6 for clarification on the integration of the eLogger hardware to the load circuit. In order to accommodate it for this particular application, a certain calibration had to be followed to maintain the accuracy of data.

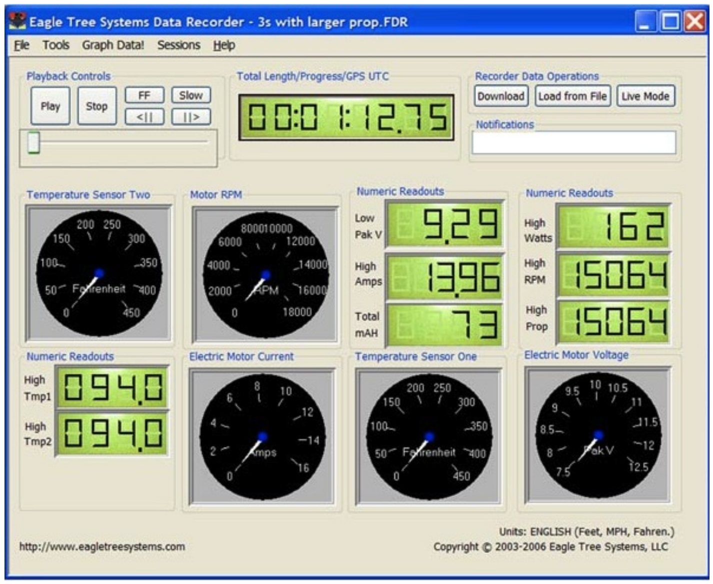

Figure 4.12: A screen shot of the live mode output dashboard on the computer screen

Depicted in Figure 4.12 is a screenshot of incoming telemetry received at the ground station about the health and generated power in the vehicle. This data is stored locally on the eLogger memory or to the computer if in live mode operation. In live mode operations, ULTRA-VNC software allows us wireless control and screen-capture of the remote computer located inside the rover.

Chapter 5

Testing

The prototype provided us with valuable data to validate the system model and to also learn more about system operation, its flaws and features. The mathematical description of the system allows for simulation of the system as well as defining basic design parameters, but the prototype will tell us much more on the rover's behaviour and impact of bouncing and other undesired states on the power generation.

5.1 Circuit Testing

This first experiment is to simulate the generated voltage with a power supply, in order to quantify losses of the charge/load circuit and to better tune some parameters related to circuitry and electronic components. The experiment will also validate the mathematical circuit model. The experiment setup consisted of a power supply that was directly connected to the charge/load circuit located in the payload box and without the generator in the circuit. The power supply was set to provide a stable voltage while the power delivered to the load in the circuit, voltage and current are continuously logged. This experiment provides good insight on the losses occurring due to the wires, rectifiers and logging equipment as well as some possible failure modes. Furthermore, the experiment also provided general information about the quality of the acquired data. In Figure 5.1

the setup of the experiment is shown.

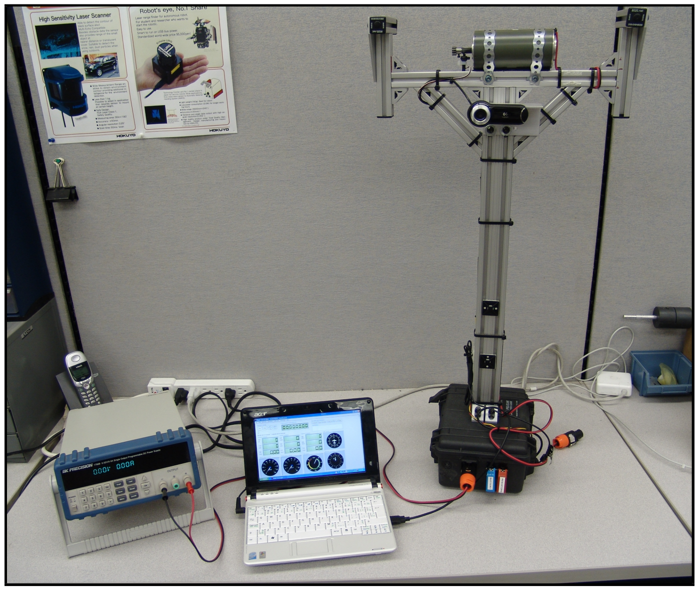

Figure 5.1: Experiment setup

The power supply provided a range of voltages that were supplied to our load circuit, which allows switching between 10 Ω, 5 Ω, 1 Ω, 0.5 Ω and a 6 volt lead-acid battery.

In Figure 5.2 we can see that the model reasonably coincides with the results acquired during the test all the way up to 6 volts. The hump that can be observed in the diagram is due to the eLogger measuring equipment. This was later confirmed by an experiment and was concluded that from 0-6 volts of delivered voltage, the current measurement of eLogger and other lab ammeters had less than 0.05 A difference while at 6 volts and further on that discrepancy increased by almost 0.12 A. This is only significant in experiments where the generator operates well above 6 volts. In most of our experiments the ball would have to travel at least 30 km/h to reach that voltage levels. This could be easily compensated with data post-processing or with a more sophisticated data-logging equipment.

This experiment partially validated the electrical model (see Figure 5.3). The next step is to complete the electrical model (M) so that the power conversion process can be

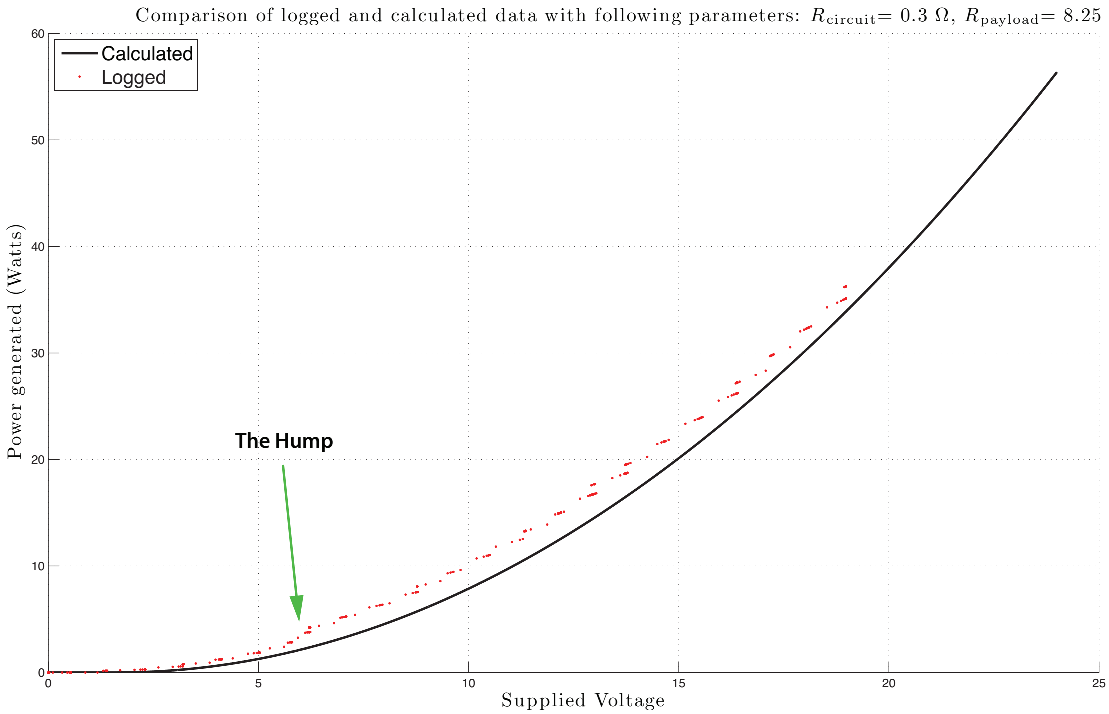

Figure 5.2: Comparison of logged and calculated data

fully understood.

5.2 Generator Testing

After validating the circuit and characterizing the generated power profile for a stable power supply output, it had to be investigated how much power can be generated with the system. This experiment validated the analytical model to establish it as a useful prediction tool for future developments. The experiment determined pendulum behaviour in a Tumbleweed vehicle rolling at different rates including pendulum displacement and power delivered to the payload.

Experimental setup can be seen in Figure 5.4). Another experiment with the pendulum hanging and supported on the mounted bearings was also perfomed. In both cases, the main axle is connected to a drill or a simple handle to rotate. Looking back for a

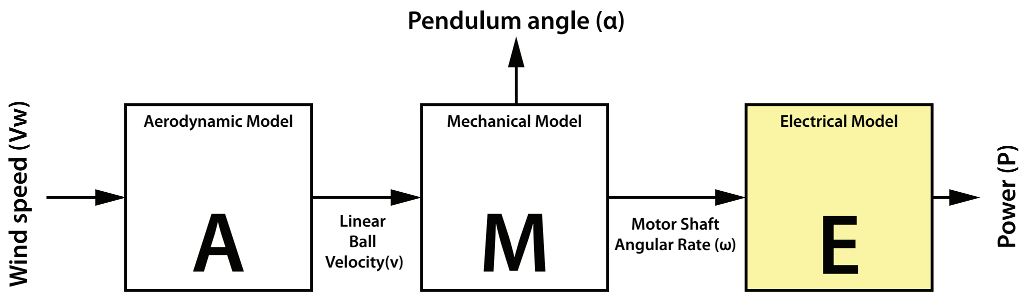

Figure 5.3: Block diagram of the parametric analytical model presented to show the progress of the model validation. In this experiment we have partially validated the electrical model (E), hence the yellow colour.

comparison with the previous experiment, the power supply has been exchanged with a motor/generator.

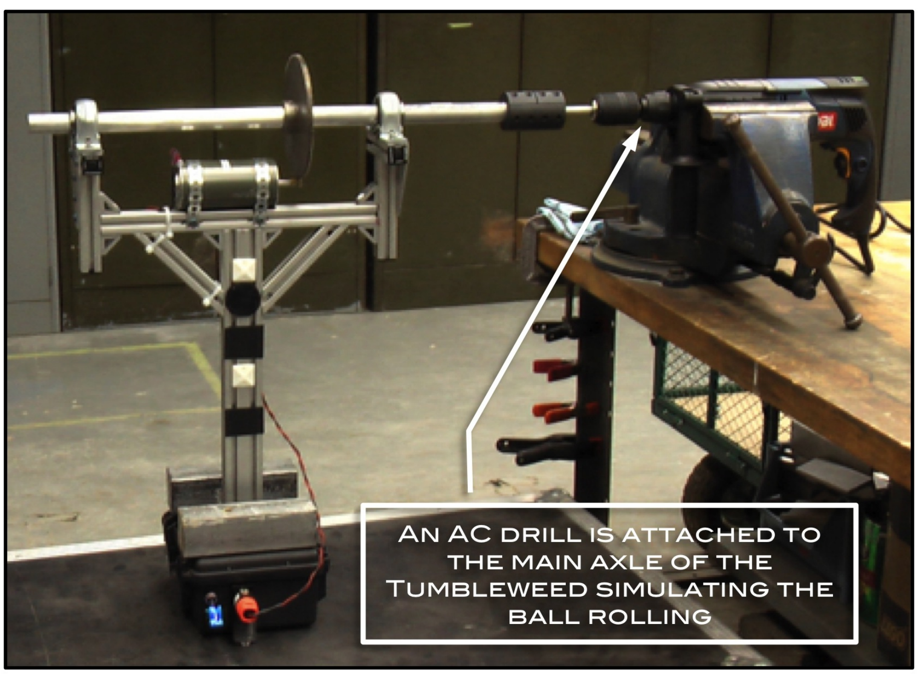

Figure 5.4: Drill test setup in which the main axle of the rover is rotated either manually or with a drill.

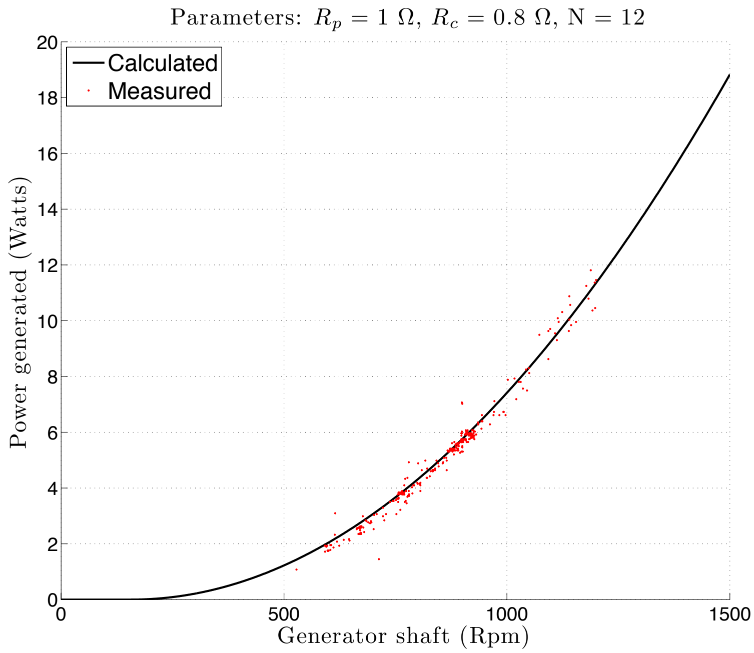

(a) Load = 1 Ω

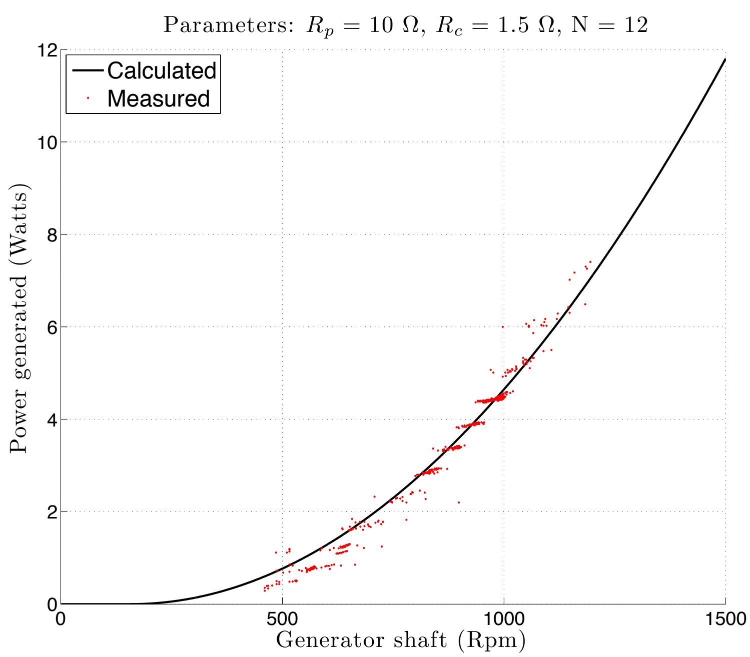

(b) Load = 10 Ω

Figure 5.5: Comparison of simulated and experimental data obtained during the experiment. Measured data displayed in red colour.

While rotating the shaft at various angular speeds, the generator will generate power and the data will be logged onto the eLogger recording device. Along with voltage and current, the speed of the shaft will also be recorded. However, due to hardware limitations, speeds lower than 450 rpm will not be recorded.

After performing the experiments, the experimental data were compared to the calculated data. Presented in Figures 5.5(a) and 5.5(b) are the diagrams of the power that was generated at various shaft speeds.

This curve comparison presented here shows that the analytical model is validated and can be used, with some fine tuning, to predict power generation performance of different Tumbleweed rover configurations.

To summarize, these indoor experiments have helped us to completely validate the electrical model, and therefore we can represent it in our block diagram (see Figure 5.6) in green colour.

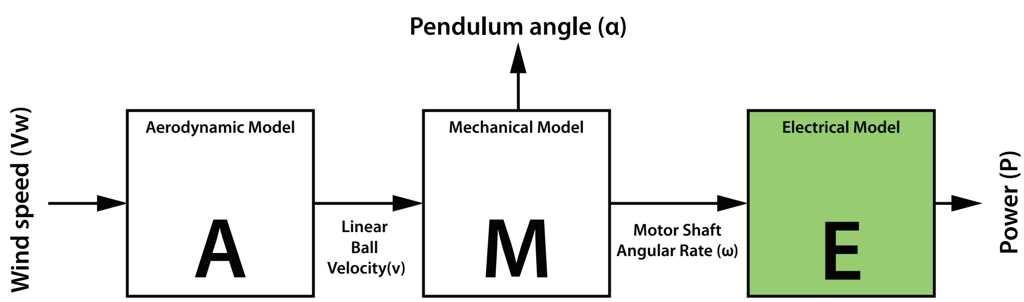

Figure 5.6: Block diagram of the parametric analytical model presented to show the progress of the model validation. In this experiment we have completed the validation of the electrical model (E), hence represented in green color.

5.3 System Readiness Test

In this set of tests, the developed system had to demonstrate complete functionality. Tests were performed on a field of approximately 5000 m^2 just outside UTIAS (see Figure 5.10). The ball was manually pushed in order to achieve different speeds and to simulate the effect of wind. In the data acquired on these preliminary field runs, it was noticed that the telemetry output (voltage, current, angular rate) is very noisy. It was necessary to characterize the source of that noise and remove it.

By analyzing the data it was determined that the primary source of that noise was due to pendulum swinging behaviour when the ball suddenly stops or accelerates. To

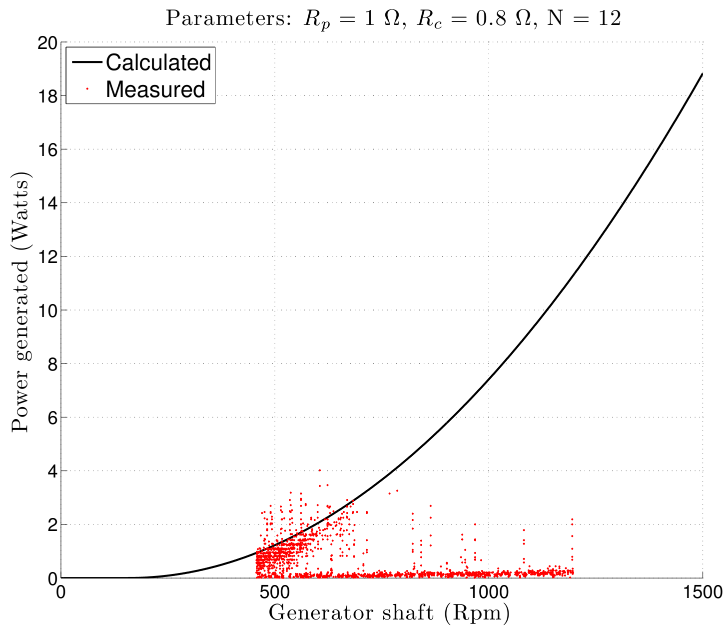

Figure 5.7: Acquired noisy data as a result of pendulum's uncontrollable swinging. This swinging behaviour produces a glitch in RPM readings with very minimal power generated.

confirm this, another pendulum bench test was performed. The main axle was rotated (manually or with a drill) while an external force was applied to the pendulum to induce swinging. This was again reflected in the noisy data, very similar to the one acquired in the field, which can be seen in Figure 5.7. In serious field operations such swinging behaviour of the pendulum could be easily stabilized with a controlled inflation/deflation sequence [25]. During the deflation the ball could be stopped and the pendulum would stop oscillating.

Furthermore, preliminary logged results in comparison with the calculated data can be seen in Figure 5.8. During the test the speed of the ball reached hardly 18 km/h, which enabled us to generate only a small amount of power as can be observed in the plot in Figure 5.8. In field operations, power generation would be recorded over a longer period of time, which would produce a much better power profile. In the next section, we will perform a set of wind experiments to finalize our system model validation and allow us to accurately calculate the effect of wind speed in our predictions.

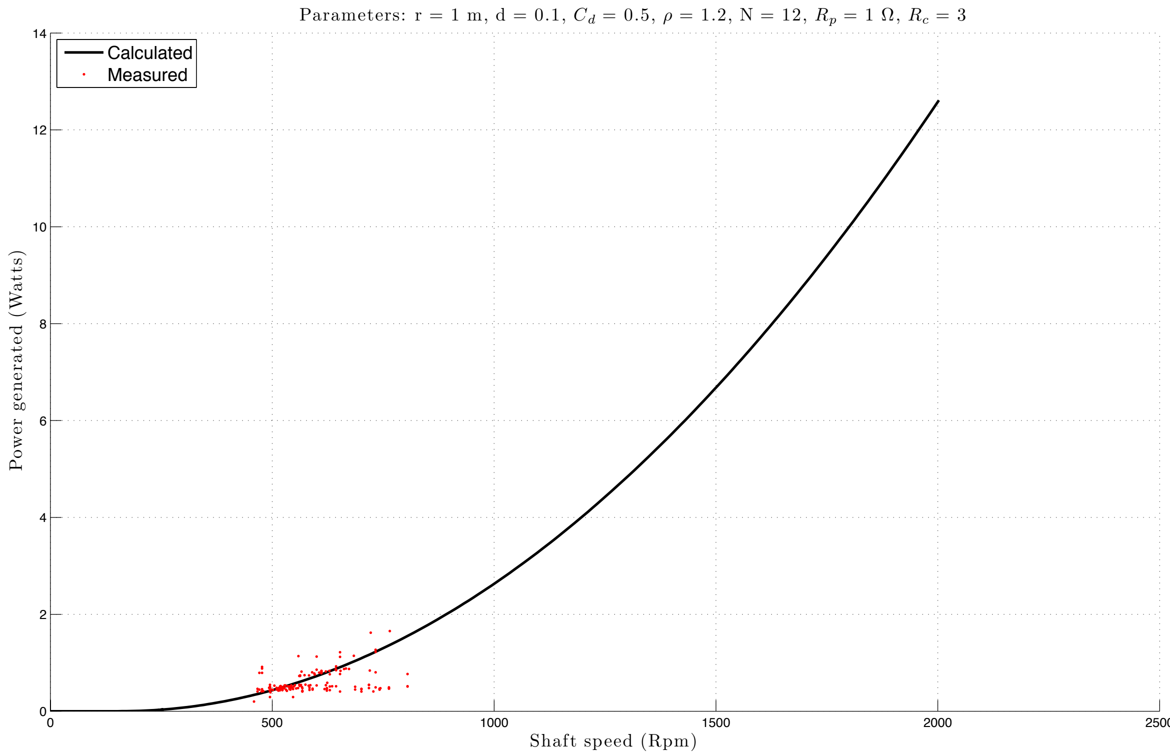

Figure 5.8: Comparison of simulated and experimental data obtained by pushing the ball across the UTIAS outdoor field with a circuit loaded with 1 Ω.

System readiness test was supposed to demonstrate the performance of the system's mechanical and structural components, as well as to confirm the relationships between the parameters of the system that directly impact power generation performance. In this experiment the mechanical model (M) was successfully validated, which is shown on our block schematic in Figure 5.9.

5.4 Wind testing

5.4.1 Testing environment

The purpose of this whole study and the development of the proof-of-concept prototype was to establish the validity of the parametric analytical model and to investigate the

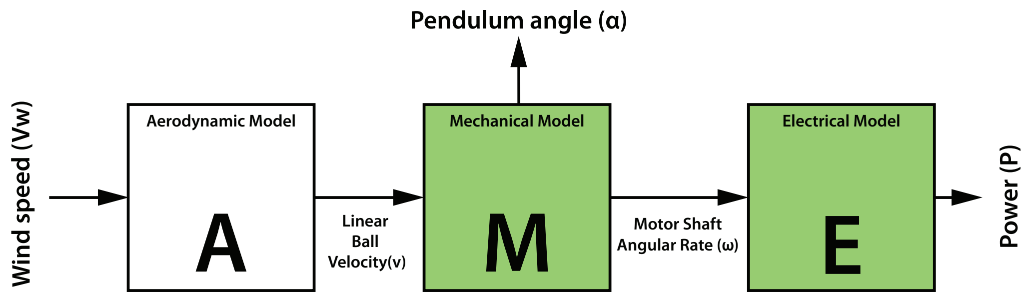

Figure 5.9: Block diagram of the parametric analytical model presented to show the progress of the model validation. In this experiment we have successfully validated the mechanical model (M).

behaviour and the capability of the system in an analogous mission scenario. Therefore, it was necessary to test the prototype and establish the impact of the wind on the rover and its power generation capabilities. Because of the logistical limitations and inability to perform the tests on an open large-area field, the prototype was tested on a 70 m long stretch of paved road in front of UTIAS. The testing area used in the experiments can be seen in Figure 5.10 shown in a white line. Performing tests on a paved road had a favourable effect due to reduced friction and damping effect on the mobility of the ball and enabling it to achieve larger acceleration, and therefore, generate more power.

5.4.2 Testing methodology

During each outdoor experiment the following had to be measured and logged:

1. Wind speed
2. Speed of the generator shaft
3. Linear velocity of the ball
4. Voltage generated

Figure 5.10: Testing environment represented. Source: Google Earth

5. Current generated

The wind speed was measured with a very simple handheld device and was recorded manually at the start of each run. Establishing precise wind speed during each run was impossible due to a hardware limitation. Voltage, current, speed of the generator shaft and linear velocity of the ball were continuously logged during each run at 4 Hz sample rate.

The tests were performed by placing the ball on the start line and waiting until the wind generated enough force to start the ball rolling. After a 70 m traverse the ball was returned to the start line and the process was repeated. After the experiments the data was downloaded from the data acquisition device. Some trial runs were also performed using a small computer installed inside the rover, which enabled on-line real time telemetry monitoring and logging.

5.4.3 Results

Approximately 10 individual experiments have been performed. Each experiment consisted of about 5 individual runs as described above. Results from only one of the experiments will be presented here. Presented on Figure 5.11 is a diagram of generated power and the linear velocity logged during the last experiment. In this experiment the ball reached almost 30 km/h in one of the runs with power yield of almost 3 Watts. Although, power generated is fairly small, these experiments provided very useful information for future consideration.

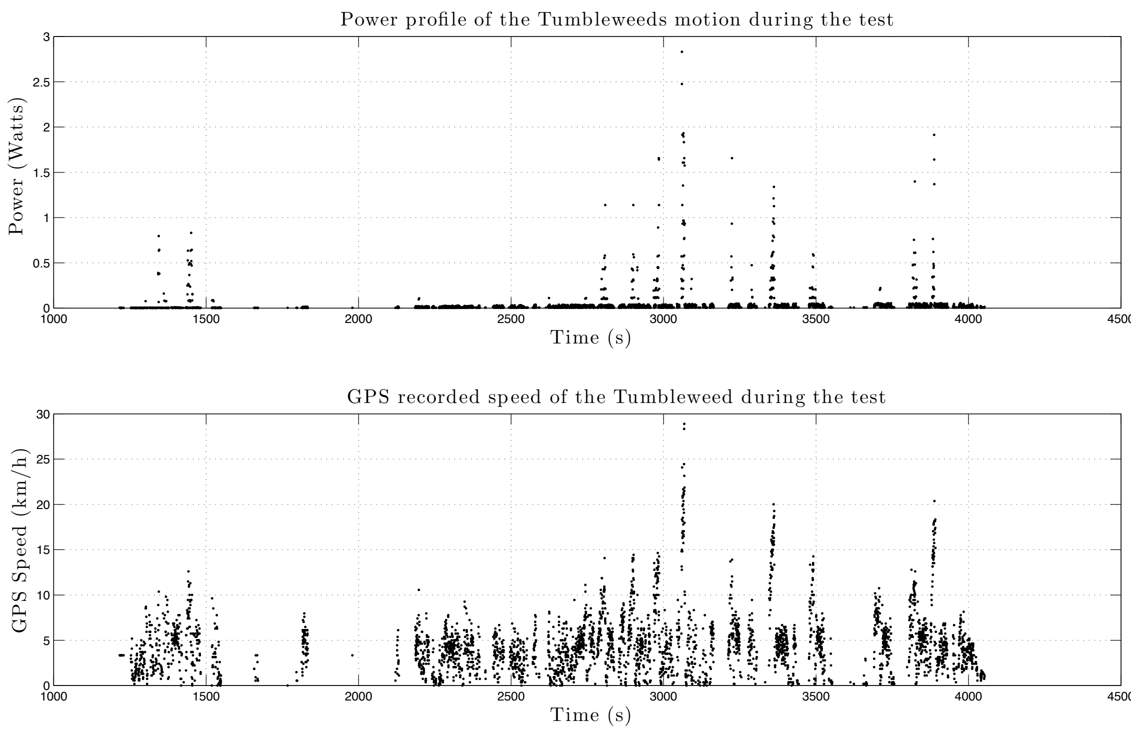

Figure 5.11: Recorded power and linear velocity of the ball during the experiment.

On the results presented in the Figure 5.12 we can establish a relationship between the speed of the wind, generator shaft speed and generated power. Due to fixed mechanical coupling between the shell and the axle of the rover, we can assume that for the given wind speed the ball is going to start rolling at a certain speed. The same relation can be assumed between the speed of the generator shaft and the generated power. On the top diagram we can see the calculated generated power in relationship to the wind speed. In the same way, on the middle diagram, a calculated relationship between the speed of the generator for a given wind speed is depicted. The bottom diagram shows the established relationship between the calculated power generated against the given speed of the generator compared to the measured values from one of the experiments. As we can see from the comparison plot, our parametric analytical model nicely validates quantifying of generated power in relation to the speed of the generator. However, we have not succeeded in validating the wind speed to the generated power. This happened for the following reasons:

1. **Impossibility of reaching quasi-static equilibrium -** Due to the very limited test area, during the experiments the ball was always accelerating and was never able to reach the constant speed, which our quasi-static model is assuming. A much larger test area would be needed in order to allow the ball to accelerate and achieve a constant velocity. Furthermore, the wind speed was also never constant during the experiments.

2. **Instability of the pendulum during rolling -** The proof-of-concept prototype also showed that the ball with a pendulum that is pushed by wind enters an unstable rolling state in which the axis of rotation changes. At that moment the ball starts to wobble and the pendulum stops generating any useful power. In further analysis, it was suggested that the moment of inertia could be much larger around the non-preferred axis of rotation. This will be studied in future work.

3. **Hardware limitations -** Due to budget restrictions it was impossible to obtain a wind speed measurement unit that could continuously record the actual wind speeds during the experiments thus making it difficult to quantify the impact of the wind on the ball.

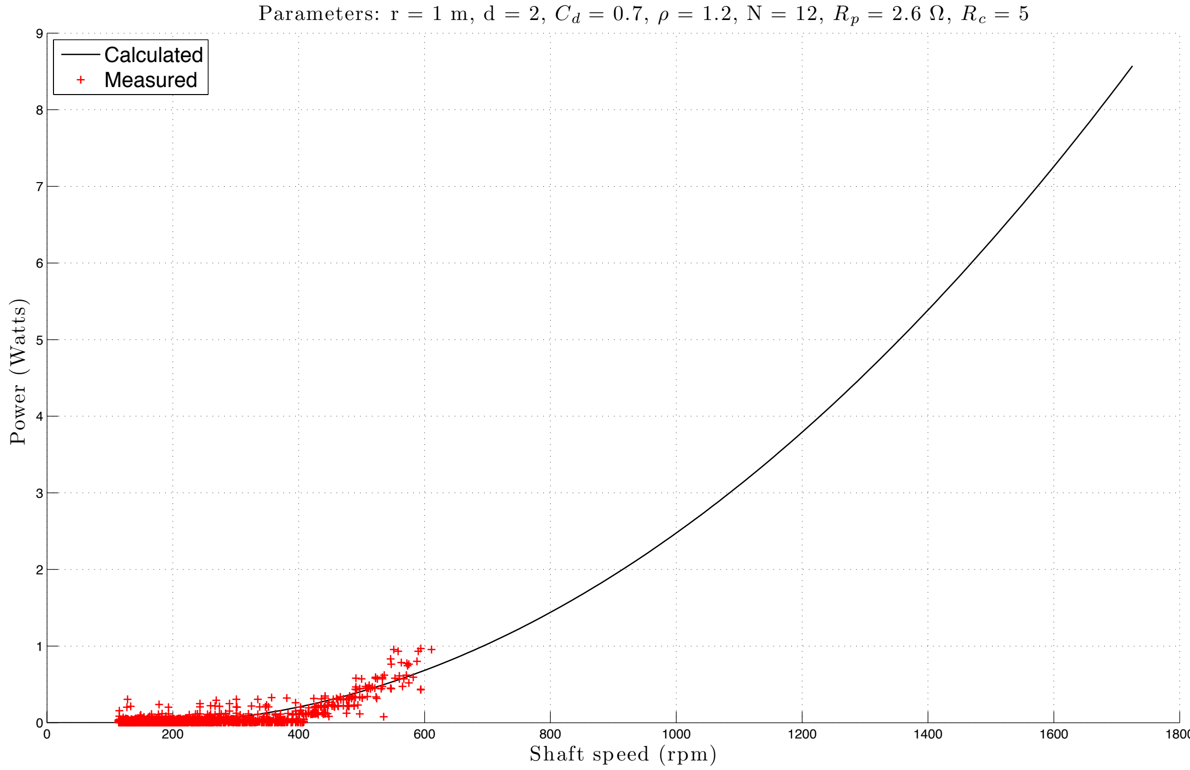

Figure 5.12: Results from the wind experiments validate again the relationship between the generator speed and power generated, but not the relationship between wind speed and the speed of the generator.

5.4.4 Conclusion and lessons learned

Although the parametric analytical model was only partially validated (shown in Figure 5.13), performing wind experiments started a whole new chapter in the development of the wind-blown spherical rovers with a pendulum. One of the most important conclusions was the discovery of rolling instability, which was not observed in dynamic simulations performed in [29], but was shown to have a great impact on the power-generation capability of the ball rover platform utilizing a single-axis pendulum mechanism. This is believed to be largely due to increased inertia about axes other than the preferred one due to heavy steel rod and aluminum extrusions used for pendulum. In [29] the rod and pendulum link were assumed to be massless. Improvement to this will be considered in future work.

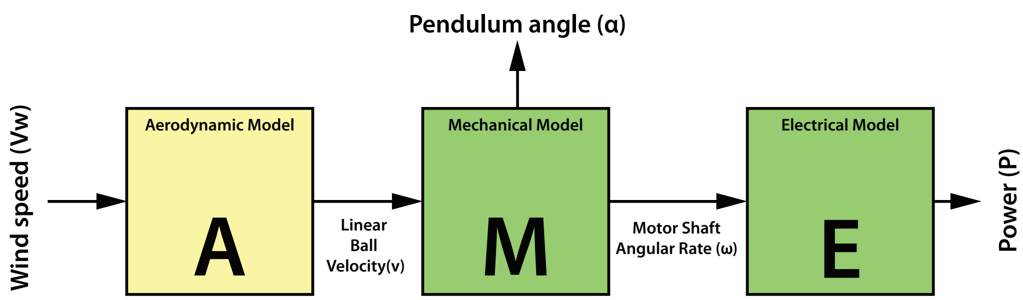

Figure 5.13: Block diagram of the parametric analytical model presented to show the progress of the model validation. In this experiment we managed, only partially, to validate the aerodynamic portion (A) of the model. The validated parts of the model are represented in green colour, while yellow represents partially validated parts of the model.

The wind test confirmed the validity of the relationship between the speed of the generator and the generated power, which gives us a good estimate on the quantity of generated power if the rolling instability is ignored. Based on that fact, we can claim that enough power can be generated in a stable-rolling Tumbleweed rover with a pendulum.

The problem of stable rolling could be addressed by development of a multi-axis pendulum platform, which would enable the pendulum to rotate about any axis thus being always stable or by introducing some novel ways of shifting the moment of inertia towards the preferred axis.

Chapter 6

Tumbleweed on Mars

In this chapter, a hypothetical mission operation will be set up on Mars. We have to determine the feasibility of power generation on the surface of Mars considering its atmospheric properties. First, we will have to consider different design parameters and how they impact the rover's performance.

6.1 Mars

6.1.1 Mission Environment

Mars has received lots of attention in the past 10 years of space exploration because it is our closest and most accessible neighbouring planet. It is located at the edge of the habitable zone of the solar system and it harbours atmosphere. For our hypothetical problem we are mostly interested in the Martian atmosphere and gravity force of the planet [2].

Compared to Earth, the atmosphere of Mars is very thin. Atmospheric pressure on the surface ranges from a low of 30 Pa (0.030 kPa) to over 1,155 Pa (1.155 kPa), with a mean pressure at the surface level of 600 Pa (0.60 kPa). As a comparison, the pressure on the surface of Mars is equal to the pressure found 35 km above the surface of Earth,

Parameters	Units	Value
Average windspeed	m/s	0 - 23
Air density	kg/m^3	0.015
Acceleration due to gravity	m/s^2	3.69
Surface pressure	kPa	0.6

Table 6.1: Environment properties of Mars significant for this hypothetical scenario

which is basically less than 1% [2].

The atmosphere on Mars consists of 95 % carbon dioxide, 3 % nitrogen, 1.6 % argon and contains traces of oxygen and water. The atmosphere is quite dusty, containing particulates about 1.5 μm in diameter which give the Martian sky a tawny colour when seen from the surface. Mars has also a much weaker gravity than Earth being only 38 % that of Earth. To summarize, Martian environment properties are given in Table 6.1 [2].

Surface winds on Mars are mostly gentle, with typical speeds of about 3 m/s. Scientists have observed wind gusts as high as 35 m/s. However, the gusts exert much less force than do equally fast winds on Earth due to lower atmospheric density [2].

During fall and winter the winds increase. At Viking Lander 1, speeds reached 27 m/s, as presented in Figure 6.1 where the original wind log is shown. It is estimated that Viking Lander 1 winds reached much higher speeds around the sol 1,720 time frame. The speed could not be calculated as the wind sensors had partial failures but the removal of piles of sand placed by the soil sampler, suggests winds of greater than 28 m/s [1].

6.1.2 Design parameter selection and comparison

Generating power on Mars would be a more challenging task than on Earth primarily because of the atmospheric properties on the Martian surface. As seen in the previous section, the atmospheric density on Mars is 1 % of Earth's. This will significantly impact the amount of wind force that will be exerted on the rover.

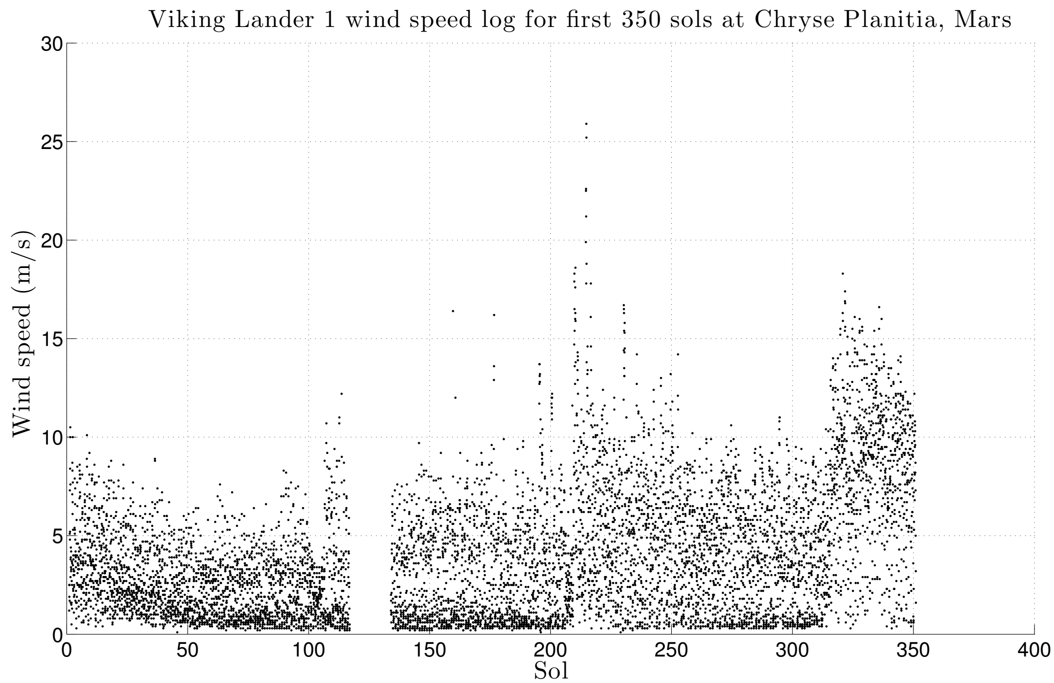

Figure 6.1: Original wind speed data from the Viking Lander recorder Chryse Planitia on Mars. Data source: [1]

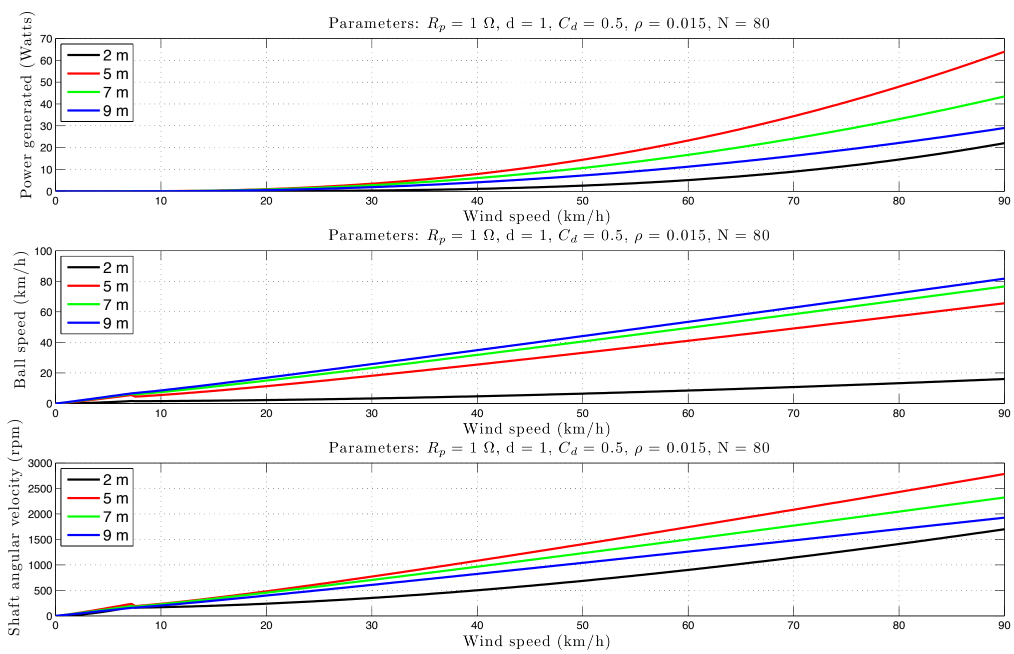

Figure 6.2: Comparison of power generated on Mars. Each line in the plot represents different ball radii, while the diagrams show the impact of wind speed to generated power, linear velocity, and the angular speed of the shaft for each of the radius.

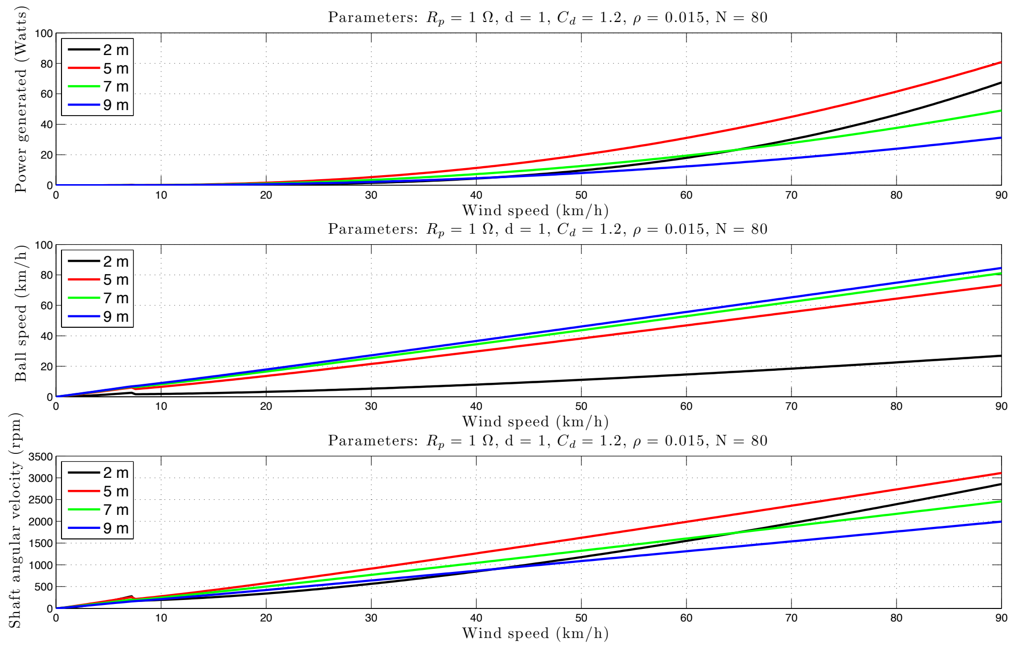

Figure 6.3: In the case with increased aid drag coefficient, the performance of Tumbleweed with smaller radius was much better. This method of increasing power generation could be utilized if Box-kite type structure would be used in the mission scenario.

If we look at Figure 6.2, we can notice that the radius of the ball on Mars would need to be much larger than the one on Earth. As we have explained in the previous sections, the power generation capability is defined by the fine balance between air density, drag, ball radius, and of course the generator used.

In order to generate as much power as we did with the configuration presented in the previous sections on Earth, a Mars Tumbleweed should be anywhere between 4 and 6 m in radius and should incorporate a much larger gear ratio than the one we currently use. This was also suggested in [4, 25, 19]. The gear ratio is still well within the permissible speed of the motor and leaves some room to safely accommodate wind speeds up to a 100 km/h. Due to its larger diameter than the ball intended for use on Earth, the ball can achieve much larger linear velocities and therefore traverse much longer paths.

We can also conclude that the radius of the ball can be significantly reduced if the drag coefficient can be increased [4, 7]. This can be done by considering a solid deployable structure in *Box kite* or *Dandellion* configurations. In Figure 6.3 it is shown that *Box kite* configuration of 2 m in radius could perform significantly better at higher wind speed than the same structure with a larger radius.

This analysis clearly showed that even a single-axis power-generating pendulum on the wind-blown spherical rover is capable of generating enough electrical power to charge a battery. Moreover, the results have shown that this is possible in the planetary environments with much thinner air densities, but with certain modifications to the design parameters.

Chapter 7

Conclusions

7.1 Thesis contributions

During this study the following contributions have been developed:

1. Introduced and partially validated a parametric analytical model, which estimates the generated power based on design parameters and environmental conditions

2. Proof-of-concept prototype of a Tumbleweed rover with a pendulum capable of generating electrical power

3. Preliminary design of a similar Tumbleweed vehicle in a Martian planetary environment

All of these contributions will provide a significant benefit to developments of similar technologies for future research efforts. Moreover, building the prototype has provided valuable information on the design of spherical vehicles and especially about specific requirements needed for wind power generation in such a vehicle. Further research should continue building on this proof of concept primarily because of the potential advantages wind-blown robots could provide for space exploration. It was shown that even with a single-axis configuration, enough power can be generated to charge a battery. The solution for power generation presented in this thesis would certainly increase autonomy and science capabilities of a wind-blown spherical mobile rover. However, there is still a lot of work to be done especially in the further evolution of the hardware to make it more reliable and stable.

7.2 Lessons learned

Wind power generation on an inflatable robot is a challenge and some general observations for the development of the future wind-blown rovers will be presented herein. During the tests, it was observed that the rolling of the ball actually produces fluctuating voltage and current outputs, which are necessary byproducts of simplifying the electronics in order to get the power outputs during experiments with as few losses as possible. In a more complex field operations scenario, a more sophisticated power system should be used that would allow a more stable power output delivered to the devices. However, this would increase the losses, which will have to be compensated by higher power yield.

Furthermore, it was also noticed how the imperfections in the shell manufacturing or uncontrolled shell pressure loss can highly impact the system's rolling stability and with that its power generation capability. If the requirements of the mission allow for smaller diameter shells, a hard, non-inflatable shell would be a better choice because complexity is reduced significantly.

This prototype was designed to prove the concept of wind power generation on a spherical rover and as such has performed quite well. During the field operations, a lot has been learned about behaviour of such a large spherical inflatable. Lack of second axis and imperfection of the spherical shell have severely impacted the stability and continuity of power generation process, which is highly impacted by the pendulum motion.

Development of this prototype also presented an important insight for better understanding of the dynamics of a single-axis pendulum spherical rovers and the rolling instabilities caused by the internal configuration of such system. As discussed earlier, this is believed to be largely due to increased inertia about axes other than the preferred one due to heavy steel rod and aluminum extrusions used for pendulum. Integration of second axis would address the problem presented, although more investigation has to be done to be confirm the underlying causes of such behaviour.

7.3 Future work

Development of a future platform would certainly benefit from the experimentation and investigation of problems such as Tumbleweed guidance, navigation, and control, payload deployment, power generation, and stability. The next generation should be focused on further hardware development to facilitate and allow several necessary improvements. These upgrades would be as follows:

- Higher performance generator
- More generators around the axes
- Power conditioning circuit with programming capabilities
- Better mechanical components that could reduce the internal friction of the system
- 3-axis pendulum for uni-directional rotation and therefore power generation and control
- Inflatable shell manufactured precisely out of high strength fibres
- More sophisticated telemetry logging device (i.e., RCATS)
- Control software and computer interface with GPS and satellite communications that allow remote operated operations

Notably, a significant focus has been put towards hardware evolution because the power generation capabilities greatly depend on the mechanical quality and optimization of the design.

The most important innovation would be the multi-axis pendulum mechanism that can be guided to any point on the sphere and therefore demonstrate power-generating capabilities on any required axis. The same pendulum mechanism could be used for controlled propulsion when no wind is present. This configuration could be integrated into both hard and inflatable shells. Generators could be integrated into any axis allowing an improved control mechanism and continuous power generation.

Research in ball rovers in general is just at its beginning and a lot more can be done. Inspired by nature, this concept also demonstrates versatility and sophistication of nature's designs that have been evolving for billions of years. We just have to keep being inspired, creative and never stop learning.

Bibliography

[1] Mars data from Viking and Mars Pathfinder missions. http://www-k12.atmos.washington.edu/k12/resources/mars_data-information/data.html.

[2] Mars Worldbook. http://www.nasa.gov/worldbook/mars_worldbook.html.

[3] Nasa Phoenix Lander Web Portal. http://phoenix.lpl.arizona.edu/index.php.

[4] Jeffrey Antol. A New Vehicle for Planetary Surface Exploration: The Mars Tumbleweed. In *1st Space Exploration Conference: Continuing the Voyage of Discovery*, number AIAA-2005-2520 in AIAA Aerospace Series. AIAA, 2005.

[5] Jeffrey Antol, Philip Calhoun, John Flick, Gregory Hajos, Richard M. Kolacinski, David Minton, Rachel Owens, and Jennifer Parker. Low Cost Mars Surface Exploration: The Mars Tumbleweed. Technical Report NASA/TM-2003-212411., NASA LaRC, August 2003.

[6] Jeffrey Antol, Richard L. Chattin, Benjamin M. Copeland, and Shawn A. Krizan. The NASA Langley Mars Tumbleweed Rover Prototype. In *44th AIAA Aerospace Sciences Meeting and Exhibit*, number AIAA 2006-64. AIAA, AIAA, January 2006.

[7] Jeffrey Antol, Steven B. Harris, Gregory A. Hajos, and Christopher V. Strickland. Wind Tunnel Tests of Evolved Mars Tumbleweed Concepts. In *44th AIAA Aerospace Sciences Meeting and Exhibit*, number AIAA-2006-69. AIAA, 2006.

[8] David Attenborough. Private life of plants. BBC DVD video.

[9] Alberto Behar, Frank Carsey, Jaret B. Matthews, and Jack A. Jones. An Antarctic Deployment of the NASA/JPL Tumbleweed Polar Rover.

[10] Alberto Behar, Frank Carsey, Jaret B. Matthews, and Jack A. Jones. NASA/JPL Tumbleweed Polar Rover. (IEEEAC paper 1003), December 2003.

[11] Fredrik Bruhn. A Spherical Inflatable Micro Robot for Planetary Exploration. *Autonomous Robotics*, 2003.

[12] R. Cecil. Mechanical toy. US Patent Office online, September 1909.

[13] J. S. Claycomb, F. R. DeJarnette, and A. P. Mazzoleni. Development and Construction of a Prototype Mars Tumbleweed Rover. In *44th AIAA Aerospace Sciences Meeting and Exhibit*, number AIAA 2006-66. AIAA, January 2006.

[14] J. M. Easterling. Toy. US Patent Office online, May 1957.

[15] G. A. Hajos, Jack A. Jones, Alberto Behar, and M. Dodd. An Overview of Wind-Driven Rovers for Planetary Exploration. AIAA.

[16] Thomas M. Hoeg, Lori Southard, Alexander Boxerbaum, Lee Reis, Jeffrey Antol, Jennifer Heldmann, and Roger D. Quinn. Tumbleweed Rover Science Mission to Dao Vallis. In *44th AIAA Aerospace Sciences Meeting and Exhibit*, number AIAA 2006-70. AIAA, 2006.

[17] Peter Jakubik, Jussi Suomela, Mika Vainio, and Tomi Ylikorpi. Biologically inspired solutions for robotic surface mobility. Final Report ARIADNA AO4532-03/6201, Helsinki University of Technology, 2004.

[18] Jack A. Jones. Inflatable Robotics for Planetary Applications. In *Proceeding of the 6th International Symposium on Artificial Intelligence and Robotics and Automation in Space: i-SAIRAS*, June 2001.

[19] Jack A. Jones. Inflatable Tumbleweed for Mars. A Presentation for the Mars Society Convention, August 2001.

[20] Urs Kafader. Maxon Motor Catalogue. Product manual, Maxon AG, 2009.

[21] R. D. Lorenz. Miniature testbeds for planetary exploration vehicles: Tumbleweed and frisbee. (IEEEAC Paper 2012), 2004.

[22] Ralph D. Lorenz, Alberto Behar, F. Nicaise, J. Jonsson, and M. Myers. Field testing and dynamic model development for a Mars Tumbleweed rover. June 2006.

[23] Ralph D. Lorenz, Jack A. Jones, and Jay J. Wu. Mars Magnetometry from a Tumbleweed Rover. Number IEEEAC paper no. 1054. IEEE AC, 2002.

[24] J. E. Martin. Radio controlled vehicle within a sphere. US Patent Office online, December 1983.

[25] Jaret B. Matthews. Development of the Tumbleweed rover. Technical report, NASA JPL, 2003.

[26] A. D. McFaul. Toy. US Patent Office online, 1918.

[27] R. W. McKeehan. Motor driven ball toy. US Patent Office online, May 1973.

[28] R. Mukherjee. Spherical mobile robot. US Patent Office online, December 1998.

[29] Forbes J R, Barfoot T D, and Damaren C J. Dynamic modeling and stability analysis of a power-generating tumbleweed rover. *Multibody System Dynamics*, (doi: 10.1007/s11044-010-9202-2), 2010.

[30] B. Shorthouse. Self-propelling device. US Patent Office online, May 1906.

[31] Lori Southard, Thomas M. Hoeg, Daniel W. Palmer, Jeffrey Antol, Richard M. Kolacinksi, and Roger D. Quinn. Exploring Mars Using a Group of Tumbleweed

Rovers. In *IEEE International Conference on Robotics and Automation*, number 1-4244-0602-1/07. IEEE, IEEE, 2007.

[32] Jussi Suomela and Tomi Ylikorpi. Ball-shaped robots: A Historical Overview and Recent Developments at TKK. *Field and Service Robotics*, STAR(25):343–354, 2006.

[33] Tomi Ylikorpi, Aarne Halme, Peter Jakubik, Jussi Suomela, and Mika Vainio. Biologically inspired solutions for robotic surface mobility. In *In Proceedings of the 8th ESA Workshop on Advanced Space Technologies for Robotics and Automation 'ASTRA 2004'*, Noordwijk, The Netherlands, 2004. ESTEC.